

Hidden charm N and Δ resonances with heavy-quark symmetry

C. García-Recio,¹ J. Nieves,² O. Romanets,³ L. L. Salcedo,¹ and L. Tolos^{4,5}

¹*Departamento de Física Atómica, Molecular y Nuclear,
and Instituto Carlos I de Física Teórica y Computacional,
Universidad de Granada, E-18071 Granada, Spain*

²*Instituto de Física Corpuscular (centro mixto CSIC-UV),
Institutos de Investigación de Paterna, Aptdo. 22085, 46071, Valencia, Spain*

³*KVI, University of Groningen, Zernikelaan 25, 9747AA Groningen, The Netherlands*

⁴*Institut de Ciències de l'Espai (IEEC/CSIC), Campus Universitat Autònoma de Barcelona,
Facultat de Ciències, Torre C5, E-08193 Bellaterra, Spain*

⁵*Frankfurt Institute for Advanced Studies,
Johann Wolfgang Goethe University, Ruth-Moufang-Str. 1, 60438 Frankfurt am Main
(Dated: February 28, 2013)*

We develop a model to describe odd parity baryon resonances generated dynamically through a unitary baryon-meson coupled-channels approach. The scheme applies to channels with light and/or heavy quark content. Distinct features of the model are that, i) the interaction is an S -wave contact one, ii) it reduces to the SU(3) Weinberg-Tomozawa Hamiltonian when light pseudoscalar mesons are involved, thus, respecting chiral symmetry, iii) spin-flavor is preserved in the light quark sector, and iv) heavy quark spin symmetry is fulfilled in the heavy quark sector. In particular, baryon-meson states with different content in c or in \bar{c} do not mix. The model is a minimal one and it contains no free parameters. In this work, we focus on baryon resonances with hidden-charm (at least one \bar{c} and one c quarks). We analyze several possible sectors and, for the sector with zero net charm, we write down the most general Lagrangian consistent with SU(3) and heavy quark spin symmetry. We explicitly study the N and Δ states, which are produced from the S -wave interaction of pseudoscalar and vector mesons with $1/2^+$ and $3/2^+$ baryons within the charmless and strangeless hidden charm sector. We predict seven odd parity N -like and five Δ -like states with masses around 4 GeV, most of them as bound states. These states form heavy-quark spin multiplets, which are almost degenerate in mass. The predicted new resonances definitely cannot be accommodated by quark models with three constituent quarks and they might be looked for in the forthcoming PANDA experiment at the future FAIR facility.

PACS numbers: 14.20.Gk 14.20.Pt 11.10.St

Contents

I. Introduction	2
II. The model	3
A. Weinberg-Tomozawa interaction	3
B. Spin-flavor extended Weinberg-Tomozawa interaction	4
C. Heavy-quark spin symmetry implementation	5
D. The model in the various sectors	8
E. Analysis of the hidden charm sectors	9
1. $C = 0$	10
2. $C = 1$	11
3. $C = 2$	11
4. $C = 3$	12
F. Lagrangian form of the interaction	13
III. Coupled-channels unitarization and symmetry breaking	16
A. Unitarization and renormalization scheme	16
B. Symmetry breaking	17
IV. Charmless and Strangeless Hidden Charm Sector: The N and Δ states	17
A. N states ($C = 0$, $S = 0$, $I = 1/2$)	18
B. Δ states ($C = 0$, $S = 0$, $I = 3/2$)	19

V. Conclusions	22
Acknowledgments	23
A. Spin-flavor states	23
B. Baryon-meson matrix elements	24
References	25

I. INTRODUCTION

The possible observation of new states with the charm degree of freedom has attracted a lot of attention over the past years in connection with many experiments such as CLEO, Belle, BaBar, and others [1–36]. Moreover, the future PANDA and CBM experiments at FAIR facility of GSI [37, 38] will aim at obtaining data in the heavy-flavor sector, thus opening the possibility for observation of new exotic states with quantum numbers of charm and strangeness. In this regard, a clear goal would be to understand the nature of these states, and in particular, whether they can be described with the usual three-quark baryon or quark-antiquark meson interpretation, or qualify better as hadron molecules within a baryon-meson coupled-channels description.

Unitarized coupled-channels approaches have shown to be very successful in describing some of the existing experimental data. These schemes include, for example, models based on the chiral perturbation amplitudes for S -wave scattering of 0^- octet Goldstone bosons off baryons of the nucleon $1/2^+$ multiplet [39–60]. Recently the charm degree of freedom has been incorporated in these models and several experimental states have been described as dynamically-generated baryon molecules [61–77]. This is the case, for example, of the $\Lambda_c(2595)$, which is the charm sector counterpart of the $\Lambda(1405)$. Some of these approaches are based on a bare baryon-meson interaction saturated with the t -channel exchange of vector mesons between pseudoscalar mesons and baryons [61–70], others make use of the Jülich meson-exchange model [71–73] or some rely on the hidden gauge formalism [74–77].

Nevertheless, these models do not explicitly incorporate heavy-quark spin symmetry (HQSS) [78–80], and therefore, it is unclear whether this symmetry is respected. HQSS is a QCD symmetry that appears when the quark masses, such as the charm mass, become larger than the typical confinement scale. HQSS predicts that all types of spin interactions involving heavy quarks vanish for infinitely massive quarks. Thus, HQSS connects vector and pseudoscalar mesons containing charmed quarks. On the other hand, chiral symmetry fixes the lowest order interaction between Goldstone bosons and other hadrons in a model independent way; this is the Weinberg-Tomozawa (WT) interaction. Thus, it is appealing to have a predictive model for four flavors including all basic hadrons (pseudoscalar and vector mesons, and $1/2^+$ and $3/2^+$ baryons) which reduces to the WT interaction in the sector where Goldstone bosons are involved and which incorporates HQSS in the sector where charm quarks participate. This model was developed in Ref. [81–83], following the steps of the SU(6) approach in the light sector of Refs. [84–87]. In these works, several resonances have been analyzed and compared to experimental states, such as the S -wave states with charm $C = 1, 2, 3$ [81, 83] together with $C = -1$ states [82]. Also this scheme has been recently extended to incorporate the bottom degree of freedom [88] in order to study the nature of the newly discovered $\Lambda_b(5912)$ and $\Lambda_b^*(5920)$ resonances [89] as possible molecular states.

In this paper we aim at continuing those studies on dynamically-generated baryon resonances using HQSS constraints. We will discuss extensively the details of the model and how heavy-quark spin symmetry is implemented. The model respects spin-flavor symmetry in the light sector and HQSS in the heavy sector, and it reduces to SU(3) WT in the light sector respecting chiral symmetry. Moreover, we will focus on the dynamical generation of hidden charmed states. The coupled-channels in the hidden charm sectors are characterized by containing equal number of c - and \bar{c} - quarks. As we shall discuss, HQSS does not mix sectors with different number of c - or \bar{c} - quarks. Thus, this model has a symmetry $SU(6) \times \text{HQSS}$, with $\text{HQSS} = SU_c(2) \times SU_{\bar{c}}(2) \times U_c(1) \times U_{\bar{c}}(1)$. We will pay a special attention to the charmless ($C = 0$) and strangeless ($S = 0$) sector. Recent works [74–77] predict the existence of a few nucleon-like states with masses around 4 GeV which result from the baryon-meson scattering in this hidden charm sector. In this paper we will analyze these results within our model, and predict the existence of several odd parity Δ - and N - like bound states with various spins. These resonances can be organized in heavy-quark spin multiplets, which are almost degenerate in mass and that can be subject to experimental detection.

The predicted new resonances might be subject to experimental detection in the forthcoming PANDA/FAIR experiment. If confirmed, they definitely cannot be accommodated by quark models with three constituent quarks.

The paper is organized as follows. In Sec. II we present the WT interaction implementing heavy-quark spin symmetry, and analyze the different hidden charm sectors, classified according to their charmed content. In Sec. III we introduce the unitarized coupled-channels approach used throughout this work. Sec. IV is devoted to present

our results and in Sec. V we summarize the conclusions. In Appendix A we give details for the construction of the meson and baryon tensors and the computation of the different matrix elements of the interaction. The tables of the interaction matrices for the different baryon-meson channels are collected in Appendix B.

II. THE MODEL

A. Weinberg-Tomozawa interaction

The theoretical model we use has been developed in previous works for baryon-meson sectors involving light and/or heavy quarks, but not for those with hidden charm, so we devote this section to fully specify the model.

The guiding principle is to blend several well established hadronic symmetries in a model as simple as possible. Specifically, to comply with chiral symmetry, $SU(N_F)_L \times SU(N_F)_R$ for N_F flavors, we require the interaction to reproduce the Weinberg-Tomozawa (WT) Hamiltonian [90–92], a contact S -wave interaction, when light pseudoscalar mesons are involved. The low energy interaction of soft pseudo-Nambu-Goldstone bosons of the spontaneously broken chiral symmetry off any (flavored) target takes the WT universal form¹

$$V_{\text{WT}} = \frac{K(s)}{4f^2} 2J_P^i J_T^i, \quad i = 1, \dots, N_F^2 - 1, \quad (2.1)$$

where f is the decay constant of the pseudoscalar meson (~ 93 MeV), and J_P^i, J_T^i are the $SU(N_F)$ group generators (with the standard normalization $f_{ikl}f_{jkl} = N_F\delta_{ij}$, where f_{ijk} are the structure constants) for pseudoscalar meson and target, respectively. Further, $K(s) = k^0 + k'^0$ represents the sum of the incoming and outgoing energies of the meson. In the center-of mass frame (CM)

$$K(s) = \frac{s - M^2 + m^2}{\sqrt{s}}, \quad (2.2)$$

where \sqrt{s} is the total CM energy, M the mass of the target, and m the mass of the pseudo-Nambu-Goldstone meson.

V_{WT} is the tree level on-shell interaction. The normalization we use is such that the corresponding T -matrix for elastic scattering is related to the scattering amplitude by

$$f(s) = -\frac{1}{8\pi} \frac{2M}{\sqrt{s}} T(s), \quad f(s) = \frac{e^{2i\delta} - 1}{2ik}, \quad (2.3)$$

where k is the CM momentum.²

For three flavors and baryons in the $\frac{1}{2}^+$ (nucleon) octet, the Hamiltonian density of the WT interaction takes the form (we assume exact $SU(3)$ symmetry for simplicity) [48]

$$\mathcal{H}_{\text{WT}}(x) = -\frac{i}{4f^2} : \text{tr} (\bar{B}\gamma^\mu [[\phi, \partial_\mu \phi], B]) : \quad (N_F = 3), \quad (2.4)$$

where ϕ and B are the meson and baryon matrices in the adjoint representation of $SU(3)$. On account of the trace cyclic property, and neglecting the meson momentum, the WT interaction can be recast as

$$\frac{i}{4f^2} : \text{tr} ([\phi, \partial_0 \phi] \{B^\dagger, B\}) : \quad (2.5)$$

From the symmetry group point of view, the interaction in Eq. (2.5) is, schematically,

$$\mathcal{H}_{\text{WT}} = \frac{1}{f^2} ((M^\dagger \otimes M)_{\text{adjoint, antisymmetric}} \otimes (B^\dagger \otimes B)_{\text{adjoint}})_{\text{singlet}}, \quad (2.6)$$

where adjoint and singlet refers to the adjoint and singlet representations of the flavor group. This corresponds with the structure in Eq. (2.1). M, M^\dagger, B and B^\dagger refer to the matrices of annihilation and creation operators of meson and baryons (see below).

¹ An extra factor 1/2 is to be added if the projectile and target are identical particles.

² $T = i\mathcal{M} = -\mathcal{T}$, \mathcal{M} and \mathcal{T} being the amplitudes defined in [93] and [94], respectively. $2MT$ equals \mathcal{M} in [95].

It is worth noticing that the eigenvalues of the relevant operator in Eq. (2.1), $2J_P^i J_T^i$, can be written using the quadratic Casimir operator of $SU(N_F)$ (see e.g. [96])

$$(2J_P^i J_T^i)_\mu = C_2(\mu; N_F) - C_2(\mu_P; N_F) - C_2(\mu_T; N_F), \quad (2.7)$$

where μ , μ_P and μ_T are, respectively, the $SU(N_F)$ irreducible representations (irreps) of the system, the Nambu-Goldstone boson (i.e., the adjoint representation) and the target. We use the normalization $C_2(\text{adjoint}; N) = N$ for $SU(N)$. In our convention a positive eigenvalue indicates repulsion and a negative one attraction.

B. Spin-flavor extended Weinberg-Tomozawa interaction

Next we turn to spin-flavor (SF) symmetry, $SU(2N_F)$, [97–99]. This symmetry has been phenomenologically successful in the classification of lowest-lying hadrons as well as in uncovering regularities present in the masses and other hadron properties [100, 101]. This is particularly true for baryons, a fact that can be understood from the large N_C (number of colors) limit of QCD. In that limit SF becomes exact for the baryon sector [102]. As for mesons, the lowest-lying states can also be classified quite naturally according to SF multiplets, but the symmetry works worse for the meson spectrum. A prime example of this is provided by the pion and rho mesons. They belong to the same multiplet of $SU(6)$ and this would require these two mesons to be approximately degenerated in mass. Also, the pion is a collective state identified as the pseudo-Nambu-Goldstone boson of the spontaneously broken approximate chiral symmetry, whereas the rho meson mass fits well with a pair of constituent quark-antiquark. Vector dominance also suggests that the rho meson should belong to the same chiral representation of the vector current $(8, 1) + (1, 8)$, which is different from the chiral representation of the pion, $(3, 3^*) + (3^*, 3)$. The apparent conflict was solved by Caldi and Pagels in two insightful papers [103, 104], where a number of related puzzles are clarified. These authors noted that chiral and SF symmetries are compatible, as they can be regarded as subgroups of a larger symmetry group, $SU(2N_F)_L \times SU(2N_F)_R$, actually a realization of the Feynman–Gell-Mann–Zweig algebra [105]. In their solution, the SF extended chiral symmetry is spontaneously broken, the rho meson being a dormant Goldstone boson of this breaking. The collective nature of the rho meson has been confirmed in lattice QCD [106]. As it is well known, exact SF invariance is not compatible with exact relativistic invariance [107]. In the Caldi-Pagels scenario, vector mesons acquire mass through SF-breaking relativistic corrections which restore Poincaré invariance.

While not an immediate consequence of the QCD Lagrangian, SF symmetry emerges in some limits, such as large N_C for baryons, as already noted, and partially also in heavy quark limits. We will turn to this point below. The lack of exact relativistic invariance is not unusual in other treatments involving hadron or quark interactions to form new hadrons, either bound states or resonances. A good example would be the successful “relativized quark model” of Isgur and coworkers [108, 109]. Similarly, in our approach the breaking of relativistic invariance is very mild: the spin is treated as just an internal label (as another kind of flavor) and our fields are effectively spinless as regards to the kinematics. So we have fully relativistic kinematics with SF as a purely internal symmetry. This entails the following. Because angular momentum can be transferred between orbital and spin components, and spin is not conserved under Lorentz transformations, a strict relativistic treatment requires fields with different spin to behave differently. In turn this yields differences in the off-shell propagators for each spin and this breaks strict SF symmetry. To the extent that we consider on-shell particles the various fields behave in the same way, and only the off-shell baryon-meson propagator (or loop function) would depend on the spin of the particles involved. We disregard this effect.³ On the other hand, because we consider pure S -wave interactions, the spin is separately conserved, and also, near threshold, the case of interest to us, the specifically relativistic properties of the spin become irrelevant. It should be noted that even approaches with formally relativistic Lagrangians are in practice subject to simplifying approximations in vertices and propagators which break exact relativistic invariance without relevant phenomenological implications. Also we remark that SF invariance is just our starting point for modeling the interaction. Modifications will be introduced below to account for other established properties of QCD, and more importantly, we use physical values for hadron masses and meson decay constants in our kinematics.

The compatibility between SF and chiral symmetries implies that the WT interaction can be extended to enjoy SF invariance, and this can be done in a unique way [84]. For the on-shell vertex the extension is simply

$$V_{\text{WT}}^{\text{sf}} = \frac{K(s)}{4f^2} 4J_M^i J_B^i, \quad i = 1, \dots, (2N_F)^2 - 1, \quad (2.8)$$

³ However, any such spin dependence would not be easy to extract from phenomenology as it will be masked by the intrinsic ambiguity of the loop function, which has to be renormalized using some phenomenological prescription.

where J_M^i and J_B^i are the $SU(2N_F)$ generators on mesons and baryons. Mesons consists of 0^- (P) and 1^- (V) lowest-lying states, while baryons contain $\frac{1}{2}^+$ (B) and $\frac{3}{2}^+$ (B^*) lowest-lying states. When this interaction is restricted to the sector $PB \rightarrow PB$ it reproduces the standard WT off B targets. Its SF extension automatically yields the standard WT for $PB^* \rightarrow PB^*$ (hence the compatibility between the two symmetries). Additionally, the extended interaction provides contact S -wave vertices for $VB \rightarrow VB$, $VB^* \rightarrow VB^*$, $PB \leftrightarrow VB$, $PB \leftrightarrow VB^*$, $PB^* \leftrightarrow VB$, $PB^* \leftrightarrow VB^*$, and $VB \leftrightarrow VB^*$. As we have tried to argue above, these new vertices are well defined predictions of an approximate emergent symmetry of hadrons. So we adopt them as our starting point to describe interactions involving vector mesons.

The Hamiltonian corresponding to the vertex in Eq. (2.8) can be written for any number of flavors and colors N_C [85]. For the physical case $N_C = 3$

$$\mathcal{H}_{\text{WT}}^{\text{sf}}(x) = -\frac{i}{4f^2} : [\Phi, \partial_0 \Phi]^A{}_B \mathcal{B}_{ACD}^\dagger \mathcal{B}^{BCD} :, \quad A, B, \dots = 1, \dots, 2N_F. \quad (2.9)$$

The indices A, B, \dots , denote spin and flavor, and so they take $2N_F$ values. $\Phi^A{}_B(x)$ is the meson field, a $2N_F \times 2N_F$ Hermitian matrix which contains the fields of 0^- (pseudoscalar) and 1^- (vector) mesons. This matrix is not traceless; for later convenience it includes the $SU(2N_F)$ singlet meson (the mathematical η_1). The contribution of η_1 to Φ is proportional to the identity matrix and so it does not couple in $\mathcal{H}_{\text{WT}}^{\text{sf}}$. The normalization of $\Phi(x)$ is such that a mass term (with a common mass m for all mesons) would read $\frac{1}{2}m^2 \text{tr}(\Phi^2)$.

$\mathcal{B}(x)$ is the baryon field. \mathcal{B}^{ABC} is a completely symmetric tensor, that is, in the irrep [3] of $SU(2N_F)$. It has 56 components for $N_F = 3$, and 120 components for $N_F = 4$, and contains the lowest-lying baryons with $J^P = \frac{1}{2}^+$ and $\frac{3}{2}^+$. The normalization of the field \mathcal{B} is such that a mass term (with a common mass M for all baryons) would take the form $M \frac{1}{3!} \mathcal{B}_{ABC}^\dagger \mathcal{B}^{ABC}$. E.g. the fields $\mathcal{B}^{123}(x)$, $\mathcal{B}^{112}(x)/\sqrt{2}$, and $\mathcal{B}^{111}(x)/\sqrt{6}$ have the standard normalization of a fermionic field. We refer to the Appendix for the detailed construction of $\Phi^A{}_B(x)$ and $\mathcal{B}^{ABC}(x)$ in terms of the individual meson and baryon fields for $N_F = 4$.

The Hamiltonian $\mathcal{H}_{\text{WT}}^{\text{sf}}$ has precisely the same structure displayed in Eq. (2.6), this time for the SF group $SU(2N_F)$.⁴

The predictions of the SF extended WT model for $N_F = 3$ have been worked out in [87] for baryonic resonances, and in [110] for the mesonic version. Applications involving charm have been given in [81–83].

Before closing this subsection, we note that the eigenvalues of the relevant operator $4J_M^i J_B^i$ in Eq. (2.8) can also be written using the quadratic Casimir operator of $SU(2N_F)$

$$(4J_M^i J_B^i)_\mu = 2(C_2(\mu; 2N_F) - C_2(\mu_M; 2N_F) - C_2(\mu_B; 2N_F)). \quad (2.10)$$

For baryons in the irrep (with Young tableau) [3] of $SU(2N_F)$ (**56** or **120** for $N_F = 3$ or 4, respectively) and mesons in $[2, 1^{2N_F-2}]$ (the adjoint representation of $SU(2N_F)$, **35** or **63** for $N_F = 3$ or 4, respectively), the baryon-meson states lie in the irreps [3], $[2, 1]$, $[5, 1^{2N_F-2}]$ and $[4, 2, 1^{2N_F-3}]$, which correspond to **56**, **70**, **700** and **1134** for $N_F = 3$, and to **120**, **168**, **2520** and **4752** for $N_F = 4$. The corresponding eigenvalues are [85]

$$\lambda_{[3]} = -4N_F, \quad \lambda_{[2,1]} = -4N_F - 6, \quad \lambda_{[5,1^{2N_F-2}]} = 6, \quad \lambda_{[4,2,1^{2N_F-3}]} = -2. \quad (2.11)$$

The SF extended WT interaction is attractive in three multiplets and repulsive in the remaining one. The sum of all eigenvalues with their multiplicity, i.e. the trace of $4J_M^i J_B^i$, is zero, as follows e.g. from $\text{tr}(J_M^i) = 0$. The operator can be written as

$$4J_M^i J_B^i = \sum_\mu \lambda_\mu P_\mu, \quad (2.12)$$

where μ are the four baryon-meson irreps of $SU(2N_F)$, λ_μ the eigenvalues and P_μ the orthogonal projectors. This allows to compute the matrix elements using the $SU(2N_F)$ Clebsch-Gordan coefficients [111].

C. Heavy-quark spin symmetry implementation

Whereas the model just described can be used directly for three flavors, the extension to include charm requires more care. One reason is that chiral symmetry and $SU(4)$ invariance are less reliable for fixing the interaction in the

⁴ Note that the singlet part in $\mathcal{B}_{ACD}^\dagger \mathcal{B}^{BCD}$ does not couple since the matrix $[\Phi, \partial_0 \Phi]$ is traceless

sectors involving charm. At the same time, new specific symmetries of non relativistic type arise when heavy quarks are involved [78–80]. In the heavy quark limit the number of charm quarks and the number of charm antiquarks are separately conserved. This implies a symmetry $U_c(1) \times U_{\bar{c}}(1)$. Likewise, the terms in the QCD Hamiltonian which depend on the heavy quark or antiquark spin are suppressed, being of order $1/m_h$, where m_h is the mass of the heavy quark. Therefore, in the heavy quark limit, arbitrary rotations of the spin carried by the c quarks and, independently, of the spin carried by the \bar{c} antiquarks, would leave unchanged the energy of the hadronic state.⁵ This implies a symmetry $SU_c(2) \times SU_{\bar{c}}(2)$ in the heavy quark limit. These invariances are aspects of heavy-quark spin symmetry (HQSS). In what follows we refer to $SU_c(2) \times SU_{\bar{c}}(2) \times U_c(1) \times U_{\bar{c}}(1)$ as the HQSS group.

The approximate HQSS reflects on the hadronic spectrum and for charm it has a level of accuracy similar to that of flavor $SU(3)$. Taking HQSS into account implies that the model described in the previous subsection, the SF extended WT or just $SU(8)$ -WT model (for four flavors), has to be slightly modified. In order to keep the model simple, we will impose exact HQSS on it. The alternative would be to introduce instead $1/m_h$ suppressions in some amplitudes, but such improvement is beyond the scope of the present work.

First, it should be noted that SF by itself already guarantees HQSS in many sectors. Consider for instance, the couplings involving the channels ND and ND^* . These channels are related through HQSS since there should be invariance under rotations of the c quark spin (leaving the light quarks unrotated), and this mixes D and D^* . But the same invariance is already implied by SF, which requires symmetry under independent rotations of spin for each flavor separately. The only cases where SF does not by itself guarantee HQSS is when there are simultaneously c quarks and \bar{c} antiquarks: SF implies invariance under equal rotations for c and \bar{c} , but HQSS requires also invariance when the two spin rotations are different.

To be more specific, let us consider baryon-meson channels, and let N_c be the number of c quarks and $N_{\bar{c}}$ the number of \bar{c} antiquarks. N_c ranges from 0 to 4, and $N_{\bar{c}}$ from 0 to 1. SF guarantees HQSS in the sectors $(N_c, N_{\bar{c}}) = (0, 0), (0, 1), (1, 0), (2, 0), (3, 0), (4, 0)$, but not in the sectors $(1, 1), (2, 1), (3, 1), (4, 1)$. As compared to the former sectors, the latter ones contain extra $c\bar{c}$ pairs. For the present discussion, we refer collectively to these sectors as sectors with “hidden charm”, regardless of whether they have net charm or not. The hidden charm sectors are the main subject of the present work. We note that, for S -wave interactions (the ones of interest here), even $SU(6)$ SF, rather than $SU(8)$, is sufficient to guarantee HQSS in the sectors without hidden charm: a rotation of the single heavy quark (or antiquark) can be produced by a light sector rotation followed by a global rotation, without changing the energy. In other words, in those sectors and for S -wave, any SF invariant interaction enjoys HQSS automatically.

It is perfectly possible to write down non trivial models enjoying simultaneously $SU(8)$ and HQSS invariances (namely, by requiring $SU_q(8) \times SU_{\bar{q}}(8)$) but they would not reduce to WT in the light sector. Concretely $SU(8)$ -WT conserves $C = N_c - N_{\bar{c}}$ but not N_c and $N_{\bar{c}}$ separately. Of course, one could impose this by hand, but it is automatically taken care of by our modified interaction below (Eq. (2.22)). Also, the restrictions of $SU(8)$ -WT to the sectors $(N_c, N_{\bar{c}}) = (1, 1), (2, 1), (3, 1), (4, 1)$ turn out to violate HQSS.

In order to implement HQSS in the model let us analyze its content. We extract the trivial kinematic part and work directly in the space with only spin and flavor as degrees of freedom. Let

$$H_{WT} = 4J_M^i J_B^i. \quad (2.13)$$

This operator can be written in terms of meson and baryon operators [81, 85], and it contains two distinct mechanisms which stem from expanding the meson commutator in Eq. (2.9),

$$\begin{aligned} H_{WT} &= H_{\text{ex}} + H_{\text{ac}}, \\ H_{\text{ex}} &= : M^A{}_C M^{\dagger C}{}_B B^{BDE} B_{ADE}^{\dagger} :, \\ H_{\text{ac}} &= - : M^{\dagger A}{}_C M^C{}_B B^{BDE} B_{ADE}^{\dagger} :, \quad A, \dots, E = 1, \dots, 2N_F. \end{aligned} \quad (2.14)$$

Here $M^A{}_B$ and B^{ABC} are the annihilation operators of mesons and baryons, respectively, with $M^{\dagger A}{}_B = (M^B{}_A)^{\dagger}$, and $B_{ABC}^{\dagger} = (B^{ABC})^{\dagger}$. B^{ABC} is a completely symmetric tensor. They are normalized as

$$\begin{aligned} [M^A{}_B, M^{\dagger C}{}_D] &= \delta_D^A \delta_B^C, \\ \{B^{ABC}, B_{A'B'C'}^{\dagger}\} &= \delta_{A'}^A \delta_{B'}^B \delta_{C'}^C + \dots \quad (6 \text{ permutations}). \end{aligned} \quad (2.15)$$

Note that in the $SU(8)$ -WT model, the η_1 ($SU(8)$ singlet meson) does not couple and could be ignored, however, this meson has to be present in the corrected interaction since it mixes with the other mesons under HQSS.

⁵ However all c quarks present in the state, being identical particles, are rotated by a common rotation, and similarly for the \bar{c} .

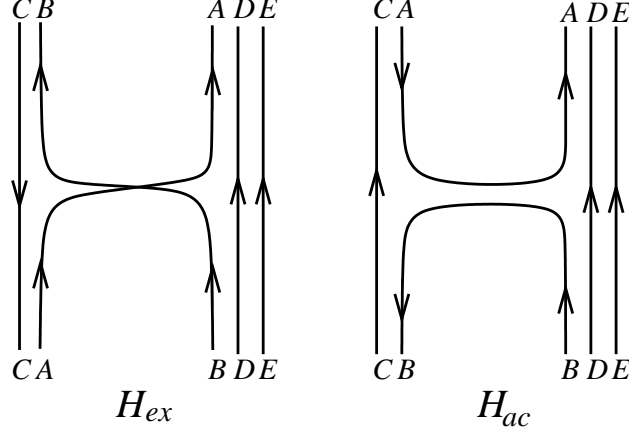


FIG. 1: The two mechanisms acting in the spin-flavor extended WT interaction. H_{ex} (exchange of quarks) and H_{ac} (annihilation and creation of quark-antiquark pairs). In the HQSS corrected version of the interaction, Eq. (2.21), the labels A and B in H_{ac} only take light-flavor values.

Schematically, representing the quark and antiquark operators by Q^A and \bar{Q}_A ,

$$M^A{}_B \sim Q^A \bar{Q}_B, \quad M^{\dagger A}{}_B \sim \bar{Q}^{\dagger A} Q_B^{\dagger}, \quad B^{ABC} \sim Q^A Q^B Q^C, \quad B^{\dagger}_{ABC} \sim Q_A^{\dagger} Q_B^{\dagger} Q_C^{\dagger}. \quad (2.16)$$

So, an upper index in M or B represents the SF of a quark to be annihilated, whereas in M^{\dagger} it represents that of an antiquark to be created. Likewise, a lower index in M^{\dagger} or B^{\dagger} represents the SF of a quark to be created while in M it represents that of an antiquark to be annihilated. From this identification it is immediate to interpret the two mechanisms H_{ex} and H_{ac} in terms of quark and antiquark propagation.

The two mechanisms involved, H_{ex} and H_{ac} are displayed in Fig. 1. In H_{ex} (exchange) the quark with spin-flavor A is transferred from the meson to the baryon, as is the quark with label B from the baryon to the meson. On the other hand, in H_{ac} (annihilation-creation) an antiquark with spin-flavor B in the meson annihilates with a similar quark in the baryon, with subsequent creation of a quark and an antiquark with spin-flavor A . In both mechanisms the quarks or antiquarks C , D and E are spectators from the point of their spin-flavor (the ubiquitous gluons are not explicated). Also in both mechanisms effectively a meson is exchanged. In passing we note that the OZI rule is automatically fulfilled as regards to the exchanged meson. OZI rule violating mechanisms would be of the type depicted in Fig. 2 and are not present in WT.

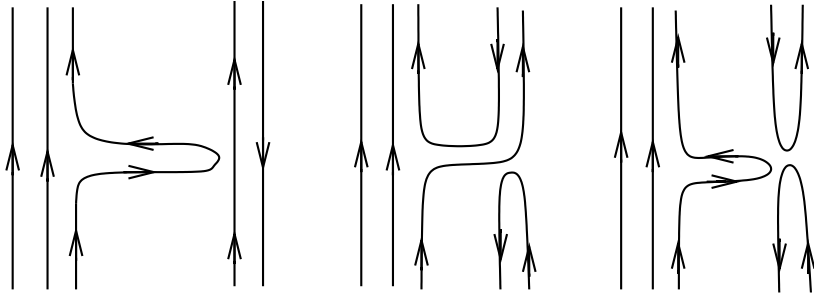


FIG. 2: OZI rule violating mechanisms. Gluons are implicit.

It appears that H_{ac} can violate HQSS when the annihilation or creation of $q\bar{q}$ pairs involves heavy quarks, whereas H_{ex} would not be in conflict with HQSS. This is indeed correct. To expose this fact more clearly, let us consider the symmetries of these two interaction mechanisms. Let $N_F = 4$ and let U be a matrix of SF $SU(8)$. Upper indices

transform with U^\dagger and lowers indices with U

$$\begin{aligned} Q^A &\rightarrow U^\dagger{}^A{}_B Q^B, & \bar{Q}^\dagger{}^A &\rightarrow U^\dagger{}^A{}_B \bar{Q}^\dagger{}^B, \\ \bar{Q}_A &\rightarrow U^B{}_A \bar{Q}_B, & Q^\dagger{}_A &\rightarrow U^B{}_A Q^\dagger{}_B. \end{aligned} \quad (2.17)$$

Therefore (with obvious matrix/tensor notation)

$$\begin{aligned} M &\rightarrow U^\dagger M U, & M^\dagger &\rightarrow U^\dagger M^\dagger U, \\ B &\rightarrow (U^\dagger \otimes U^\dagger \otimes U^\dagger) B, & B^\dagger &\rightarrow B^\dagger (U \otimes U \otimes U). \end{aligned} \quad (2.18)$$

The indices are so contracted that H_{ex} and H_{ac} are both invariant under these $\text{SU}(8)$ transformations. However, HQSS requires also invariance when the charm quark and the charm antiquark receive different rotations. To examine this, let us consider the transformation under $U \in \text{SU}_q(8)$ and $\bar{U} \in \text{SU}_{\bar{q}}(8)$, i.e., different transformations for quarks and antiquarks (previously $U = \bar{U}$). In this case

$$Q \rightarrow U^\dagger Q, \quad \bar{Q}^\dagger \rightarrow \bar{U}^\dagger \bar{Q}^\dagger, \quad \bar{Q} \rightarrow \bar{Q} \bar{U}, \quad Q^\dagger \rightarrow Q^\dagger U, \quad (2.19)$$

and therefore

$$\begin{aligned} M &\rightarrow U^\dagger M \bar{U}, & M^\dagger &\rightarrow \bar{U}^\dagger M^\dagger U, \\ B &\rightarrow (U^\dagger \otimes U^\dagger \otimes U^\dagger) B, & B^\dagger &\rightarrow B^\dagger (U \otimes U \otimes U). \end{aligned} \quad (2.20)$$

Clearly, the mechanism H_{ex} , which depends on the combination MM^\dagger , is still invariant under this larger group $\text{SU}_q(8) \times \text{SU}_{\bar{q}}(8)$.⁶ It certainly preserves SF and HQSS. On the other hand, H_{ac} depends on the combination $M^\dagger M$ which transforms with \bar{U} , while BB^\dagger transforms with U . H_{ac} is SF invariant ($U = \bar{U}$) but not HQSS invariant. A simple solution to enforce HQSS with minimal modifications is to remove just the offending contributions in H_{ac} , which come from creation or annihilation of charm quark-antiquark pairs. This implies to remove the interaction when the labels A or B are of heavy type in H_{ac} .⁷ That is, we adopt the following modified version of the H_{ac} mechanism

$$H'_{\text{ac}} = - : M^{\dagger\hat{A}}{}_C M^C{}_{\hat{B}} B^{\hat{B}DE} B^\dagger_{\hat{A}DE} :, \quad C, D, E = 1, \dots, 8, \quad \hat{A}, \hat{B} = 1, \dots, 6. \quad (2.21)$$

The indices with hat are restricted to $\text{SU}(6)$. By construction N_c and $N_{\bar{c}}$ are exactly conserved in H'_{ac} . Also $\text{SU}_c(2) \times \text{SU}_{\bar{c}}(2)$ is conserved: when U and \bar{U} act only on the heavy sector $M^{\dagger\hat{A}}{}_C M^C{}_{\hat{B}}$ and $B^{\hat{B}DE} B^\dagger_{\hat{A}DE}$ are unchanged. So HQSS is preserved. On the other hand, when $U = \bar{U}$ and this matrix acts on the light sector, H'_{ac} is unchanged, so it enjoys $\text{SU}(6)$ symmetry. Exact SF $\text{SU}(8)$ and flavor $\text{SU}(4)$ is no longer present. Presumably this breaking of $\text{SU}(4)$ is comparable to the breaking through the kinematics due to the substantially heavier mass of the charmed quark.

To summarize, our model (in all sectors) is given by

$$V = \frac{K(s)}{4f^2} H'_{\text{WT}}, \quad H'_{\text{WT}} = H_{\text{ex}} + H'_{\text{ac}}. \quad (2.22)$$

This model fulfills some desirable requirements: i) It has symmetry $\text{SU}(6) \times \text{HQSS}$, i.e., SF symmetry in the light sector and HQSS in the heavy sector, the two invariances being compatible. ii) It reduces to $\text{SU}(6)$ -WT in the light sector, so it is consistent with chiral symmetry in that sector. And, iii) is a minimal modification that preserves simplicity and does not introduce new adjustable parameters.

D. The model in the various sectors

We can analyze the model in the different $(N_c, N_{\bar{c}})$ sectors, which as already noted, do not mix due to HQSS.

In all the sectors without hidden charm, namely, $(N_c, N_{\bar{c}}) = (0, 1), (0, 0), (1, 0), (2, 0), (3, 0), (4, 0)$, H'_{ac} produces the same amplitudes as H_{ac} when the latter is restricted to the corresponding sector. Indeed these interactions vanish

⁶ Note that the commutation relations Eq. (2.15) are also preserved by this symmetry.

⁷ Keeping the contributions with $A = B$ of heavy type would preserve $\text{U}_c(1) \times \text{U}_{\bar{c}}(1)$, i.e., conservation of N_c and $N_{\bar{c}}$, but not $\text{SU}_c(2) \times \text{SU}_{\bar{c}}(2)$.

unless the state contains a quark-antiquark pair with quark and antiquark of the same type. In the absence of hidden charm, the pair must be light and in this case the two operators produce the same result. This is consistent with our previous observation that, when there are only heavy quarks or heavy antiquarks but not both, SF already implies HQSS. So in all these sectors, our model produces the same amplitudes as SU(8)-WT after removing channels involving hidden charm. This observation has been applied in [81–83, 88].

It is noteworthy that, in the sectors $(N_c, N_{\bar{c}}) = (0, 1)$ and $(4, 0)$, corresponding to $C = -1$ and $C = 4$, $H'_{ac} = H_{ac} = 0$ as they do not contain light quark-antiquark pairs. Also these two sectors cannot couple to any other $(N_c, N_{\bar{c}})$ sector in the baryon-meson case. Therefore for them, our model coincides directly with SU(8)-WT.

Let us turn now to the sectors with hidden charm. These are $(N_c, N_{\bar{c}}) = (1, 1), (2, 1), (3, 1), (4, 1)$. For all these sectors H'_{ac} vanishes. The reason is that in these sectors the relevant quark-antiquark pair (quark and antiquark with equal labels) is necessarily of heavy type, and such amplitude has been removed from H'_{ac} . (Note that H_{ac} does not vanish in these sectors.) So for the hidden charm sectors H'_{WT} reduces to the exchange mechanism H_{ex} .

The interaction is effectively H_{ex} for the four hidden charm sectors and also for $C = -1$ and $C = 4$. This has the immediate consequence that the interaction H'_{WT} has only two eigenvalues, namely -2 (attractive) and 6 (repulsive), in those sectors.⁸ This follows from the fact that H_{ex} has a large (accidental) symmetry group, $SU_q(8) \times SU_{\bar{q}}(8)$, which produces only two large multiplets of degenerated states in the baryon-meson coupled-channels space. Under $SU_q(8) \times SU_{\bar{q}}(8)$ the baryons fall in the irrep $(\mathbf{120}, \mathbf{1})$ ($\mathbf{120}$ being the symmetric representation of three quarks with 8 possible spin-flavor states).⁹ Likewise, the mesons belong to $(\mathbf{8}, \mathbf{8}^*)$ (being $q\bar{q}$ states). Therefore, the baryon-meson states form two $SU_q(8) \times SU_{\bar{q}}(8)$ multiplets:

$$(\mathbf{120}, \mathbf{1}) \otimes (\mathbf{8}, \mathbf{8}^*) = (\mathbf{330}, \mathbf{8}^*) \oplus (\mathbf{630}, \mathbf{8}^*), \quad (2.23)$$

($\mathbf{330}$ is the symmetric representation [4] of SU(8) while $\mathbf{630}$ corresponds to the mixed symmetry [3, 1]). The two corresponding eigenvalues are¹⁰

$$\lambda_{(\mathbf{330}, \mathbf{8}^*)} = 6, \quad \lambda_{(\mathbf{630}, \mathbf{8}^*)} = -2. \quad (2.24)$$

These two eigenvalues are also present in the original SU(8)-WT interaction (namely, $\lambda_{\mathbf{2520}} = 6$ and $\lambda_{\mathbf{4752}} = -2$ from Eq. (2.11)) since the two interactions coincide for $C = -1$ or $C = 4$. It can also be noted that under SF SU(8), these multiplets reduce as follows

$$(\mathbf{330}, \mathbf{8}^*) = \mathbf{120} \oplus \mathbf{2520}, \quad (\mathbf{630}, \mathbf{8}^*) = \mathbf{120} \oplus \mathbf{168} \oplus \mathbf{4752}. \quad (2.25)$$

Of course, these are the same SU(8) irreps obtained from $\mathbf{120} \otimes \mathbf{63}$ (baryon-meson except η_1) and $\mathbf{120} \otimes \mathbf{1}$ (baryon- η_1). Therefore, the interaction can be written using SU(8) Clebsch-Gordan coefficients by means of¹¹

$$H_{ex} = 6(P'_{\mathbf{120}} + P_{\mathbf{2520}}) - 2(P_{\mathbf{120}} + P_{\mathbf{168}} + P_{\mathbf{4752}}). \quad (2.26)$$

We emphasize that the large multiplets $(\mathbf{330}, \mathbf{8}^*)$ and $(\mathbf{630}, \mathbf{8}^*)$ are not realized in our model. First of all, they contain sectors without hidden charm, for which the interaction does not reduce to the exchange mechanism H_{ex} . And second, the eigenvalues 6 and -2 refer only to the driving operator $4J_M^i J_B^i$. The vertex V in Eq. (2.22) depends also on hadron masses and meson decay constants, for which we use physical values in V and in the propagators. The values that we use for these magnitudes are collected in Table II of [83].

E. Analysis of the hidden charm sectors

Here we consider hidden charm sectors with $C = 0, 1, 2, 3$, i.e. $N_{\bar{c}} = 1$ and $N_c = 1, 2, 3, 4$, respectively. We want to classify the possible states under the symmetry group $SU(6) \times \text{HQSS}$, with $\text{HQSS} = SU_c(2) \times SU_{\bar{c}}(2) \times U_c(1) \times U_{\bar{c}}(1)$. Since in the hidden charm sectors there is exactly one heavy antiquark, it is not necessary to specify the irrep of the factor $SU_{\bar{c}}(2) \times U_{\bar{c}}(1)$ and we can use the notation $\mathbf{R}_{2J_c+1, C}$ for the irreps of $SU(6) \times \text{HQSS}$, \mathbf{R} being the SU(6) irrep of the light sector, C the charm quantum number and J_c the total spin carried by the one or more c quarks (not

⁸ Remarkably, these two eigenvalues are the only N_F -independent ones in Eq. (2.11).

⁹ Fermi-Dirac statistic is taken care of by the antisymmetric color wavefunction.

¹⁰ They can be obtained by applying H_{ex} to two suitable states, e.g., $(M^{\dagger 1}_1 B^{\dagger}_{211} \pm M^{\dagger 1}_2 B^{\dagger}_{111})|0\rangle$.

¹¹ One exception comes from the two $\mathbf{120}$ irreps, which differ by the type of symmetry of the four quarks. This information is not contained in the SU(8) Clebsch-Gordan coefficients.

including the spin of the \bar{c} antiquarks). The corresponding dimension is $\dim \mathbf{R} \times (2J_c + 1) \times 2$ (the last factor coming from the two possible spin states of the \bar{c}).

Subsequently, we study the breaking of light SF down to $SU(3) \times SU(2)$ keeping HQSS, and enumerate the number of attractive channels in each (C, \mathbf{r}, J) sector, where \mathbf{r} is the $SU(3)$ irrep and J the total spin.

In practice we will assume exact isospin and spin $SU(2)_I \times SU(2)_J$, as well as conservation of each flavor, but not exact $SU(3)$ and HQSS, for the baryons and mesons composing the coupled-channels space. Therefore the sectors are labeled by (C, S, I, J) , S being the strangeness quantum number and I the isospin. This implies a further breaking of each (C, \mathbf{r}, J) sector into (C, S, I, J) subsectors.

1. $C = 0$

For $C = 0$, the quark content is $\ell\ell c\bar{c}$, with two possibilities of grouping into baryon-meson: $(\ell\ell)(c\bar{c})$ and $(\ell\ell c)(\bar{c})$. (Here ℓ denotes any light flavor quark, u, d, s .) The total dimension of the space is $56 \times 2 \times 2 + 21 \times 2 \times 6 \times 2 = 728$, and contains the following $SU(6) \times \text{HQSS}$ multiplets¹²

$$\mathcal{H}_{C=0} = \mathbf{56}_{2,0} \oplus \mathbf{56}_{2,0} \oplus \mathbf{70}_{2,0} \quad (SU(6) \times \text{HQSS}). \quad (2.27)$$

The eigenvalues turn out to be

$$\lambda_{\mathbf{56}_{2,0}} = \lambda_{\mathbf{70}_{2,0}} = -2, \quad \lambda'_{\mathbf{56}_{2,0}} = 6. \quad (2.28)$$

The accidental degeneracy between $\mathbf{70}_{2,0}$ and one $\mathbf{56}_{2,0}$ takes place in our model and it is not a necessary consequence of $SU(6) \times \text{HQSS}$. This symmetry does not fix the three possible eigenvalues and the precise splitting between the two copies of $\mathbf{56}_{2,0}$. In general, the accidental degeneracy will be lifted in V and the T -matrix even when an exact $SU(6) \times \text{HQSS}$ invariance is assumed in the hadron masses and meson decay constants.

Next, we consider the breaking of light SF $SU(6)$ down to $SU(3) \times SU_{J_\ell}(2)$. E.g. $\mathbf{56} = \mathbf{8}_2 \oplus \mathbf{10}_4$. HQSS is unbroken. After recoupling the spin carried by light and heavy quarks and antiquarks to yield the total spin J , we obtain representations of $SU(3) \times SU(2)_J$ labeled as \mathbf{r}_{2J+1} , where \mathbf{r} is the $SU(3)$ irrep. This yields the following reductions (the two $\mathbf{56}_{2,0}$ have the same reduction)

$$\begin{aligned} \mathbf{56}_{2,0} &= (\mathbf{8}_2 \oplus \mathbf{10}_4)_{2,0} = (\mathbf{8}_2 \oplus \mathbf{8}_2 \oplus \mathbf{8}_4) \oplus (\mathbf{10}_2 \oplus \mathbf{10}_4 \oplus \mathbf{10}_4 \oplus \mathbf{10}_6), \\ \mathbf{70}_{2,0} &= (\mathbf{1}_2 \oplus \mathbf{8}_2 \oplus \mathbf{8}_4 \oplus \mathbf{10}_2)_{2,0} = (\mathbf{1}_2 \oplus \mathbf{1}_2 \oplus \mathbf{1}_4) \oplus (\mathbf{8}_2 \oplus \mathbf{8}_2 \oplus \mathbf{8}_4) \oplus (\mathbf{8}_2 \oplus \mathbf{8}_4 \oplus \mathbf{8}_4 \oplus \mathbf{8}_6) \oplus (\mathbf{10}_2 \oplus \mathbf{10}_2 \oplus \mathbf{10}_4). \end{aligned} \quad (2.29)$$

In the reduction $(\mathbf{8}_2)_{2,0} = (\mathbf{8}_2 \oplus \mathbf{8}_2 \oplus \mathbf{8}_4)$ in $\mathbf{56}_{2,0}$, the three octets only differ in how the light sector spin is coupled to the heavy sector spin, therefore these three irreps are degenerated if exact HQSS is assumed. $(\mathbf{8}_2 \oplus \mathbf{8}_2 \oplus \mathbf{8}_4)$ is a multiplet of $SU(3) \times \text{HQSS}$. Similar statements hold in the other cases: each $\mathbf{56}_{2,0}$ produces two such multiplets and $\mathbf{70}_{2,0}$ produces four. Consequently, in the hidden charm sector with $C = 0$ we expect to find 8 different eigenvalues after $SU(6) \times \text{HQSS}$ is broken down to $SU(3) \times \text{HQSS}$. Let λ_1, λ_2 be the eigenvalues of the two multiplets in the repulsive $\mathbf{56}_{2,0}$, λ_3, λ_4 in the attractive $\mathbf{56}_{2,0}$, and $\lambda_5, \lambda_6, \lambda_7, \lambda_8$ those in $\mathbf{70}_{2,0}$. In this case, the spectra in each (C, \mathbf{r}, J) sector is as follows:

$$\begin{aligned} \mathbf{1}_2 &: (\lambda_5, \lambda_5), \\ \mathbf{1}_4 &: (\lambda_5), \\ \mathbf{8}_2 &: (\lambda_1, \lambda_1, \lambda_3, \lambda_3, \lambda_6, \lambda_6, \lambda_7), \\ \mathbf{8}_4 &: (\lambda_1, \lambda_3, \lambda_6, \lambda_7, \lambda_7), \\ \mathbf{8}_6 &: (\lambda_7), \\ \mathbf{10}_2 &: (\lambda_2, \lambda_4, \lambda_8, \lambda_8), \\ \mathbf{10}_4 &: (\lambda_2, \lambda_2, \lambda_4, \lambda_4, \lambda_8), \\ \mathbf{10}_6 &: (\lambda_2, \lambda_4). \end{aligned} \quad (2.30)$$

In the $SU(6)$ limit, $\lambda_1 = \lambda_2, \lambda_3 = \lambda_4, \lambda_5 = \lambda_6 = \lambda_7 = \lambda_8$. Breaking down the symmetry to $SU(3)$, one expects

$$\lambda_{3,4,5,6,7,8} < 0 < \lambda_{1,2}. \quad (2.31)$$

¹² $(\ell\ell\ell)(c\bar{c})$ is purely $\mathbf{56}_{2,0}$ from the symmetry of the three light quarks. The two light quarks in $(\ell\ell c)$ are symmetric giving a $\mathbf{21}$ of $SU(6)$, coupled to the further light quark in (\bar{c}) gives $\mathbf{21} \otimes \mathbf{6} = \mathbf{56} \oplus \mathbf{70}$. These two $\mathbf{56}_{2,0}$ are not directly those in Eq. (2.28).

Each negative eigenvalue can give rise to a resonance or bound state. Each such state is a full multiplet of $SU(3) \times SU(2)_J$. This implies the following expected number of states in each (C, \mathbf{r}, J) sector: up to two states in $\mathbf{1}_2$, one in $\mathbf{1}_4$, five in $\mathbf{8}_2$, four in $\mathbf{8}_4$, one in $\mathbf{8}_6$, three in $\mathbf{10}_2$, three in $\mathbf{10}_4$, and one in $\mathbf{10}_6$, all of them with $C = 0$.

2. $C = 1$

For $C = 1$ there are two baryon-meson structures, namely, $(\ell c)(c\bar{c})$ and $(\ell cc)(\ell\bar{c})$. The total dimension of the space is 384, with the following reduction under $SU(6) \times \text{HQSS}$

$$\mathcal{H}_{C=1} = \mathbf{21}_{3,1} \oplus \mathbf{21}_{3,1} \oplus \mathbf{21}_{1,1} \oplus \mathbf{15}_{3,1} \quad (SU(6) \times \text{HQSS}), \quad (2.32)$$

and eigenvalues

$$\lambda_{\mathbf{21}_{3,1}} = \lambda_{\mathbf{21}_{1,1}} = \lambda_{\mathbf{15}_{3,1}} = -2, \quad \lambda'_{\mathbf{21}_{3,1}} = 6. \quad (2.33)$$

Once again the accidental degeneracy beyond $SU(6) \times \text{HQSS}$ is lifted in the T -matrix.

After the breaking $SU(6) \supset SU(3) \times SU(2)_{J_\ell}$, and recoupling to J , one finds

$$\begin{aligned} \mathbf{21}_{3,1} &= (\mathbf{6}_3 \oplus \mathbf{3}_1^*)_{3,1} = (\mathbf{6}_2 \oplus \mathbf{6}_2 \oplus \mathbf{6}_4 \oplus \mathbf{6}_4 \oplus \mathbf{6}_6) \oplus (\mathbf{3}_2^* \oplus \mathbf{3}_4^*), \\ \mathbf{21}_{1,1} &= (\mathbf{6}_3 \oplus \mathbf{3}_1^*)_{1,1} = (\mathbf{6}_2 \oplus \mathbf{6}_4) \oplus (\mathbf{3}_2^*), \\ \mathbf{15}_{3,1} &= (\mathbf{6}_1 \oplus \mathbf{3}_3^*)_{3,1} = (\mathbf{6}_2 \oplus \mathbf{6}_4) \oplus (\mathbf{3}_2^* \oplus \mathbf{3}_2^* \oplus \mathbf{3}_4^* \oplus \mathbf{3}_4^* \oplus \mathbf{3}_6^*). \end{aligned} \quad (2.34)$$

Thus for $C = 1$, each of the four $SU(6)$ irreps split into two $SU(3) \times \text{HQSS}$ multiplets.¹³

In principle there are eight different eigenvalues. Denoting by λ_1, λ_2 the eigenvalues of the two multiplets in the repulsive $\mathbf{21}_{3,1}$, λ_3, λ_4 for the attractive $\mathbf{21}_{3,1}$, λ_5, λ_6 for $\mathbf{21}_{1,1}$, and λ_7, λ_8 for $\mathbf{15}_{3,1}$, the spectra in each (C, \mathbf{r}, J) sector is as follows:

$$\begin{aligned} \mathbf{3}_2^* &: (\lambda_2, \lambda_4, \lambda_6, \lambda_8, \lambda_8), \\ \mathbf{3}_4^* &: (\lambda_2, \lambda_4, \lambda_8, \lambda_8), \\ \mathbf{3}_6^* &: (\lambda_8), \\ \mathbf{6}_2 &: (\lambda_1, \lambda_1, \lambda_3, \lambda_3, \lambda_5, \lambda_7), \\ \mathbf{6}_4 &: (\lambda_1, \lambda_1, \lambda_3, \lambda_3, \lambda_5, \lambda_7), \\ \mathbf{6}_6 &: (\lambda_1, \lambda_3). \end{aligned} \quad (2.35)$$

In the $SU(6)$ limit, $\lambda_1 = \lambda_2$, $\lambda_3 = \lambda_4$, $\lambda_5 = \lambda_6$, and $\lambda_7 = \lambda_8$. If only $SU(3)$ symmetry is assumed, we expect the following number of states: up to four states in $\mathbf{3}_2^*$, three in $\mathbf{3}_4^*$, one in $\mathbf{3}_6^*$, four in $\mathbf{6}_2$, four in $\mathbf{6}_4$, and one in $\mathbf{6}_6$.

3. $C = 2$

For the hidden charm sector with $C = 2$ there are two baryon-meson quark structures, $(\ell cc)(c\bar{c})$ and $(ccc)(\ell\bar{c})$. The space has dimension 120, with the following reduction and eigenvalues:

$$\begin{aligned} \mathcal{H}_{C=2} &= \mathbf{6}_{2,2} \oplus \mathbf{6}_{4,2} \oplus \mathbf{6}_{4,2} \quad (SU(6) \times \text{HQSS}) \\ \lambda_{\mathbf{6}_{2,2}} &= \lambda_{\mathbf{6}_{4,2}} = -2, \quad \lambda'_{\mathbf{6}_{4,2}} = 6. \end{aligned} \quad (2.36)$$

The $SU(3) \times \text{HQSS}$ multiplets are as follows:

$$\begin{aligned} \mathbf{6}_{2,2} &= (\mathbf{3}_2)_{2,2} = (\mathbf{3}_2 \oplus \mathbf{3}_2 \oplus \mathbf{3}_4), \\ \mathbf{6}_{4,2} &= (\mathbf{3}_2)_{4,2} = (\mathbf{3}_2 \oplus \mathbf{3}_4 \oplus \mathbf{3}_4 \oplus \mathbf{3}_6). \end{aligned} \quad (2.37)$$

¹³ Note that the two $(\mathbf{6}_2 \oplus \mathbf{6}_4)$ multiplets above do not mix if HQSS holds, as they carry different heavy quark spin labels. Such label has been left implicit to avoid clumsiness.

In this case the $SU(6) \times HQSS$ multiplets are not reduced further under $SU(3) \times HQSS$. Calling λ_1 the eigenvalue of the repulsive $\mathbf{6}_{4,2}$, λ_2 that of the attractive $\mathbf{6}_{4,2}$, and λ_3 the one of $\mathbf{6}_{2,2}$, yields the following spectra for the three (C, \mathbf{r}, J) sectors:

$$\begin{aligned}\mathbf{3}_2 &: (\lambda_1, \lambda_2, \lambda_3, \lambda_3), \\ \mathbf{3}_4 &: (\lambda_1, \lambda_1, \lambda_2, \lambda_2, \lambda_3), \\ \mathbf{3}_6 &: (\lambda_1, \lambda_2).\end{aligned}\tag{2.38}$$

This produces the following expected maximum number of states: three in $\mathbf{3}_2$, three in $\mathbf{3}_4$ and one in $\mathbf{3}_6$

It can be noted in the present case, $C = 2$ with hidden charm, the assumption of $SU(6)$ invariance does not add anything (does not reduce the number of parameters) on top of that of $SU(3)$. The reason is that here $HQSS$ automatically implies SF: there is just one light quark and rotations of it can be produced by combining global rotations with heavy quark rotations.

4. $C = 3$

For $C = 3$ there is just one quark structure, $(ccc)c\bar{c}$. The dimension is 16. The $SU(6) \times HQSS$ reduction is

$$\mathcal{H}_{C=3} = \mathbf{1}_{3,3} \oplus \mathbf{1}_{5,3} \quad (SU(6) \times HQSS),\tag{2.39}$$

with eigenvalues

$$\lambda_{\mathbf{1}_{3,3}} = -2, \quad \lambda_{\mathbf{1}_{5,3}} = 6.\tag{2.40}$$

The $SU(3) \times SU(2)_J$ reduction is:

$$\begin{aligned}\mathbf{1}_{3,3} &= (\mathbf{1}_1)_{3,3} = (\mathbf{1}_2 \oplus \mathbf{1}_4), \\ \mathbf{1}_{5,3} &= (\mathbf{1}_1)_{5,3} = (\mathbf{1}_4 \oplus \mathbf{1}_6).\end{aligned}\tag{2.41}$$

Once again, the $SU(6) \times HQSS$ multiplets are not reduced further under $SU(3) \times HQSS$.

The following spectra is obtained for the various (C, \mathbf{r}, J) sectors

$$\begin{aligned}\mathbf{1}_2 &: (\lambda_2), \\ \mathbf{1}_4 &: (\lambda_1, \lambda_2), \\ \mathbf{1}_6 &: (\lambda_1),\end{aligned}\tag{2.42}$$

where λ_1 denotes the eigenvalue corresponding to $\mathbf{1}_{5,3}$, and λ_2 that of $\mathbf{1}_{3,3}$. So no states will be produced in $\mathbf{1}_6$, and up to one state is expected in $\mathbf{1}_2$ and $\mathbf{1}_4$.

Some of the results of this subsection are summarized in Table I.

	C	0			1		2	3
J	$SU(3)$	$\mathbf{1}$	$\mathbf{8}$	$\mathbf{10}$	$\mathbf{3}^*$	$\mathbf{6}$	$\mathbf{3}$	$\mathbf{1}$
$1/2$		2	7	4	5	6	4	1
		(2)	(5)	(3)	(4)	(4)	(3)	(1)
$3/2$		1	5	5	4	6	5	2
		(1)	(4)	(3)	(3)	(4)	(3)	(1)
$5/2$		0	1	2	1	2	2	1
		(0)	(1)	(1)	(1)	(1)	(1)	(0)

TABLE I: Total number of channels for each J and each $SU(3)$ irrep, for the various hidden charm sectors. Here each channel represents a full $SU(3)$ and spin multiplet (C, \mathbf{r}, J) (rather than a isospin-spin multiplet, (C, S, I, J) .) The expected number of resonances in each sector is shown between parenthesis. The actual number of resonances will depend on the values of the physical masses and meson decay constants.

F. Lagrangian form of the interaction

In the strict heavy quark limit, the total spin J , and the separate spins of the light, heavy quarks and heavy antiquarks subsystems are conserved, when only S -wave interactions are considered. Moreover, the matrix elements of QCD Hamiltonian depend only on the spin-flavor quantum numbers of the light degrees of freedom. Each n -fold degenerated $SU(6)$ or $SU(3)$ multiplet implies the specification of $n(n+1)/2$ parameters which are coupling constants of the corresponding operators present in the interaction. From the previous analysis it follows that the number of independent operators in the hidden charm sectors with $C = 0, 1, 2, 3$ is 4, 5, 4, 2, respectively, for a generic interaction if $SU(6) \times \text{HQSS}$ invariance is assumed and 12, 10, 4, 2 if the symmetry is reduced to $SU(3) \times \text{HQSS}$.

In what follows we will focus on the sector with hidden charm and $C = 0$. For this sector we will write down the most general (modulo kinematical factors) S -wave Lagrangian consistent with $SU(3) \times \text{HQSS}$ for the baryon-meson coupled-channels space. This Lagrangian contains 12 operators and our model gives well defined values for the corresponding coupling constants. We should note that we actually compute the matrix elements of our interaction using directly the previous expressions, either in terms of projectors using Clebsch-Gordan coefficients, or of hadron creation and annihilation operators in spin-flavor space, by taking Wick contractions. Nevertheless, writing the interaction in field-theoretical Lagrangian form is highly interesting in order to make contact with alternative approaches in the literature.

For this purpose it is convenient to organize the hadrons forming multiplets of HQSS into building blocks with well defined HQSS transformation properties [80, 112–114]. Specifically, consider a HQSS doublet composed of pseudoscalar meson and vector meson with one heavy quark (e.g. D and D^*). Let $M^{(c)}$ and $M_\mu^{(c)}$ be the corresponding fields, then

$$\begin{aligned} \mathbf{M}^{(c)} &= Q_+(M_\mu^{(c)(+)}\gamma^\mu + M^{(c)(+)}\gamma_5), \\ \overline{\mathbf{M}}^{(c)} &= \gamma_0 \mathbf{M}^{(c)\dagger}\gamma_0 = (M_\mu^{(c)\dagger(-)}\gamma^\mu - M^{(c)\dagger(-)}\gamma_5)Q_+. \end{aligned} \quad (2.43)$$

As usual (\pm) represent the positive and negative frequency part of the fields, corresponding to purely annihilation for $(+)$ and purely creation for $(-)$. Therefore, $\mathbf{M}^{(c)}$ [$\overline{\mathbf{M}}^{(c)}$] annihilates [creates] the meson with one heavy quark but it does not create [annihilate] the corresponding antimeson with a heavy antiquark. A similar proviso is applied in all the other fields for hadrons carrying heavy quarks and/or antiquarks. Besides,

$$Q_\pm = \frac{1 \pm \not{v}}{2} \quad (2.44)$$

where v^μ is the heavy hadron velocity ($v^2 = 1$). We use Bjorken and Drell [115] conventions for the Dirac gammas. For the hadron fields we use the conventions of [111] and this fixes the relative sign between pseudoscalar and vector (see Appendix A).

Likewise, for a HQSS meson doublet with one heavy antiquark

$$\begin{aligned} \mathbf{M}^{(\bar{c})} &= (M_\mu^{(\bar{c})(+)}\gamma^\mu + M^{(\bar{c})(+)}\gamma_5)Q_-, \\ \overline{\mathbf{M}}^{(\bar{c})} &= \gamma_0 \mathbf{M}^{(\bar{c})\dagger}\gamma_0 = Q_-(M_\mu^{(\bar{c})\dagger(-)}\gamma^\mu - M^{(\bar{c})\dagger(-)}\gamma_5). \end{aligned} \quad (2.45)$$

For a HQSS meson doublet with one heavy quark and one heavy antiquark (e.g., η_c and J/ψ):

$$\begin{aligned} \mathbf{M}^{(c\bar{c})} &= Q_+(M_\mu^{(c\bar{c})(+)}\gamma^\mu + M^{(c\bar{c})(+)}\gamma_5)Q_-, \\ \overline{\mathbf{M}}^{(c\bar{c})} &= \gamma_0 \mathbf{M}^{(c\bar{c})\dagger}\gamma_0 = Q_-(M_\mu^{(c\bar{c})\dagger(-)}\gamma^\mu - M^{(c\bar{c})\dagger(-)}\gamma_5)Q_+. \end{aligned} \quad (2.46)$$

For a HQSS baryon doublet with exactly one heavy quark (e.g., Σ_c and Σ_c^*),

$$\begin{aligned} \mathbf{B}^{(c)\mu} &= B^{(c)\mu(+)} + \frac{1}{\sqrt{3}}(\gamma^\mu + v^\mu)\gamma_5 B^{(c)(+)}, \\ \overline{\mathbf{B}}^{(c)\mu} &= B^{(c)\dagger\mu}\gamma_0 = \overline{B}^{(c)\mu(-)} + \frac{1}{\sqrt{3}}\overline{B}^{(c)(-)}(\gamma^\mu - v^\mu)\gamma_5. \end{aligned} \quad (2.47)$$

Here $B^{(c)}$ is the Dirac spinor of the $1/2^+$ baryon in the doublet while $\overline{B}^{(c)\mu}$ is the Rarita-Schwinger field for the $3/2^+$ baryon: $v_\mu B^{(c)\mu} = \gamma_\mu B^{(c)\mu} = 0$.

Finally, for a HQSS singlet baryon with exactly one heavy quark (e.g., Λ_c)

$$\mathbf{B}^{(c)} = B^{(c)(+)}, \quad \overline{\mathbf{B}}^{(c)} = B^{(c)\dagger}\gamma_0 = \overline{B}^{(c)(-)}. \quad (2.48)$$

In addition, the polarization of the baryons carrying heavy quarks is such that $Q_- B^{(c)(+)} = Q_- B^{(c)\mu(+)} = 0$, hence

$$Q_- B^{(c)} = Q_- B^{(c)\mu} = 0. \quad (2.49)$$

Under HQSS rotations these fields transform as follows

$$\begin{aligned} S_c M^{(c)}, \quad M^{(\bar{c})} S_c^{-1}, \quad S_c M^{(c\bar{c})} S_c^{-1}, \quad S_c B^{(c)}, \quad S_c B^{(c)\mu} \\ \overline{M}^{(c)} S_c^{-1}, \quad S_{\bar{c}} \overline{M}^{(\bar{c})}, \quad S_{\bar{c}} \overline{M}^{(c\bar{c})} S_c^{-1}, \quad \overline{B}^{(c)} S_c^{-1}, \quad \overline{B}^{(c)\mu} S_c^{-1}. \end{aligned} \quad (2.50)$$

Here S_c and $S_{\bar{c}}$ are the matrices in Dirac space representing the c or \bar{c} spin rotation and satisfy $S_{c,\bar{c}}^\dagger = \gamma_0 S_{c,\bar{c}}^{-1} \gamma_0$.

All other hadrons without heavy quarks nor antiquarks are HQSS singlets. They have complete fields (positive and negative frequency parts) and are denoted without boldface type.

The hadrons are also organized into SU(3) multiplets. We use fields with labels $a, b, c, \dots = 1, 2, 3$ (or up, down, strange) in the fundamental or anti-fundamental representations of SU(3), in such a way that

$$T_{b,\dots}^{a,\dots} \rightarrow U^\dagger{}^a{}_{a'} U^{b'}{}_b \dots T_{b',\dots}^{a',\dots}, \quad U \in \text{SU}(3) \quad (2.51)$$

For $C = 0$ with hidden charm, the following SU(3) multiplets are needed

$$\bar{D}^a = \left(\bar{D}^0 \quad \bar{D}^- \quad \bar{D}_s \right) \quad (2.52)$$

Here \bar{D}^0 represents the HQSS doublet formed by \bar{D}^0 and \bar{D}^{*0} , etc.

$$\Sigma_c^{\mu ab} = \begin{pmatrix} \sqrt{2} \Sigma_c^{\mu++} & \Sigma_c^{\mu+} & \Xi_c^{\mu+} \\ \Sigma_c^{\mu+} & \sqrt{2} \Sigma_c^{\mu 0} & \Xi_c^{\mu 0} \\ \Xi_c^{\mu+} & \Xi_c^{\mu 0} & \sqrt{2} \Omega_c^\mu \end{pmatrix} \quad (2.53)$$

This is a symmetric tensor (irrep **6** of SU(3)). Σ_c^μ , Ξ_c^μ , and Ω_c^μ are the HQSS doublets with (Σ_c, Σ_c^*) , (Ξ_c', Ξ_c^*) , and (Ω_c, Ω_c^*) , respectively.

$$\Xi_{ca} = \left(-\Xi_c^0 \quad \Xi_c^+ \quad -\Lambda_c \right) \quad (2.54)$$

In this case the members of the SU(3) multiplet are HQSS singlets. Further we define ψ as the SU(3) singlet and HQSS doublet containing $(\eta_c, J/\psi)$.

In addition, the following light baryon multiplets appear: with $J^P = 1/2^+$

$$\Sigma^a{}_b = \begin{pmatrix} \frac{1}{\sqrt{6}}\Lambda - \frac{1}{\sqrt{2}}\Sigma^0 & \Sigma^+ & -p \\ -\Sigma^- & \frac{1}{\sqrt{6}}\Lambda + \frac{1}{\sqrt{2}}\Sigma^0 & -n \\ -\Xi^- & \Xi^0 & -\sqrt{\frac{2}{3}}\Lambda \end{pmatrix}, \quad (2.55)$$

and with $J^P = 3/2^+$, Δ_μ^{abc} , a Rarita-Schwinger field and a symmetric tensor normalized as

$$\begin{aligned} \Delta_\mu^{111} &= \sqrt{6} \Delta_\mu^{++}, \quad \Delta_\mu^{112} = \sqrt{2} \Delta_\mu^+, \quad \Delta_\mu^{122} = \sqrt{2} \Delta_\mu^0, \quad \Delta_\mu^{222} = \sqrt{6} \Delta_\mu^-, \\ \Delta_\mu^{113} &= \sqrt{2} \Sigma_\mu^{*+}, \quad \Delta_\mu^{123} = \Sigma_\mu^{*0}, \quad \Delta_\mu^{223} = \sqrt{2} \Sigma_\mu^{*-}, \\ \Delta_\mu^{133} &= \sqrt{2} \Xi_\mu^{*0}, \quad \Delta_\mu^{233} = \sqrt{2} \Xi_\mu^{*-}, \\ \Delta_\mu^{333} &= \sqrt{6} \Omega_\mu. \end{aligned} \quad (2.56)$$

The relative phases of all fields here are standard with respect to the conventions adopted in [111] for the rotation, flavor and spin-flavor groups. So for instance, (Ξ_c^+, Ξ_c^0) is a standard isospin doublet and $(\Sigma^+, \Sigma^0, \Sigma^-)$ is a standard isovector. For SU(3) (and SU(4)) the convention in [116] is used instead of that in [117].¹⁴

¹⁴ The matrix elements between standard states of the step operators $u \leftrightarrow d$, $d \leftrightarrow s$, and $s \leftrightarrow c$ are required to be non negative [116], rather than those of $u \leftrightarrow d$ and $u \leftrightarrow s$ [117].

Regarding parity, we note that the hadrons with spin-parity 1^- or $1/2^+$ have normal parity, whereas those with 0^- or $3/2^+$ have abnormal parity. So Σ_a^b , ψ , Ξ_{ca} , and \bar{D}^a are true tensors while Δ_μ^{abc} , and Σ_{cab}^μ are pseudotensors. Also, Σ_a^b , Ξ_{ca} , Δ_i^{abc} , and Σ_{cab}^i have large upper components while ψ and \bar{D}^a have large off-diagonal blocks in Dirac space. The γ_5 matrices introduced to preserve parity fit in this scheme.

Next, we write down the 12 most general operators allowed by $SU(3) \times \text{HQSS}$ in the baryon-meson coupled-channels space, in S -wave and preserving parity. The operator $\overleftrightarrow{\partial}_v = v^\mu (\overrightarrow{\partial}_\mu - \overleftarrow{\partial}_\mu)$ acts on the mesons only and it is introduced in order to produce the correct kinematical dependence in the amplitudes.

$$\mathcal{L}_1(x) = g_1 \bar{\Sigma}_a^b \Sigma_a^b \text{tr}(\bar{\psi} i \overleftrightarrow{\partial}_v \psi), \quad (2.57)$$

$$\mathcal{L}_2(x) = g_2 \frac{1}{3!} \bar{\Delta}_{abc}^\mu \Delta_\mu^{abc} \text{tr}(\bar{\psi} i \overleftrightarrow{\partial}_v \psi), \quad (2.58)$$

$$\mathcal{L}_3(x) = g_3 \bar{\Xi}_c^a \psi (-i \overleftrightarrow{\partial}_v) \bar{D}_b \Sigma_a^b + \text{h.c.}, \quad (2.59)$$

$$\mathcal{L}_4(x) = g_4 \epsilon^{bcd} \bar{\Sigma}_{cab}^\mu \psi (-i \overleftrightarrow{\partial}_v) \bar{D}_c \gamma_\mu \gamma_5 \Sigma_d^a + \text{h.c.}, \quad (2.60)$$

$$\mathcal{L}_5(x) = g_5 \frac{1}{2} \bar{\Sigma}_{cab}^\mu \psi (-i \overleftrightarrow{\partial}_v) \bar{D}_c \Delta_\mu^{abc} + \text{h.c.}, \quad (2.61)$$

$$\mathcal{L}_6(x) = g_6 \bar{\Xi}_c^a \Xi_{ca} \text{tr}(\bar{D}_b i \overleftrightarrow{\partial}_v \bar{D}^b), \quad (2.62)$$

$$\mathcal{L}_7(x) = g_7 \bar{\Xi}_c^a \Xi_{cb} \text{tr}(\bar{D}_a i \overleftrightarrow{\partial}_v \bar{D}^b), \quad (2.63)$$

$$\mathcal{L}_8(x) = g_8 \epsilon^{bcd} \bar{\Sigma}_{cab}^\mu \Xi_{cd} \text{tr}(\bar{D}_c \gamma_\mu \gamma_5 i \overleftrightarrow{\partial}_v \bar{D}^a) + \text{h.c.}, \quad (2.64)$$

$$\mathcal{L}_9(x) + \mathcal{L}_{10}(x) = \frac{1}{2} \bar{\Sigma}_{cab}^\mu \Sigma_c^{\nu ab} \text{tr}(\bar{D}_c (g_9 g_{\mu\nu} + g_{10} i \sigma_{\mu\nu}) i \overleftrightarrow{\partial}_v \bar{D}^c), \quad (2.65)$$

$$\mathcal{L}_{11}(x) + \mathcal{L}_{12}(x) = \bar{\Sigma}_{cab}^\mu \Sigma_c^{\nu bc} \text{tr}(\bar{D}_b (g_{11} g_{\mu\nu} + g_{12} i \sigma_{\mu\nu}) i \overleftrightarrow{\partial}_v \bar{D}^a). \quad (2.66)$$

The traces refer to Dirac space.

The reduction of these Lagrangians when no strangeness is involved is as follows:

$$\mathcal{L}_1(x) = g_1 \bar{N} N \text{tr}(\bar{\psi} i \overleftrightarrow{\partial}_v \psi), \quad (2.67)$$

$$\mathcal{L}_2(x) = g_2 \bar{\Delta}^\mu \Delta_\mu \text{tr}(\bar{\psi} i \overleftrightarrow{\partial}_v \psi), \quad (2.68)$$

$$\mathcal{L}_3(x) = g_3 \bar{\Lambda}_c \psi (-i \overleftrightarrow{\partial}_v) \bar{D} N + \text{h.c.}, \quad (2.69)$$

$$\mathcal{L}_4(x) = g_4 \bar{\Sigma}_{cj}^\mu \psi (-i \overleftrightarrow{\partial}_v) \bar{D} \tau_j \gamma_\mu \gamma_5 N + \text{h.c.}, \quad (2.70)$$

$$\mathcal{L}_5(x) = \sqrt{3} g_5 \bar{\Sigma}_{cj}^\mu \bar{\psi} (-i \overleftrightarrow{\partial}_v) \psi T_j \Delta_\mu + \text{h.c.}, \quad (2.71)$$

$$\mathcal{L}_6(x) = g_6 \bar{\Lambda}_c \Lambda_c \text{tr}(\bar{D} i \overleftrightarrow{\partial}_v \bar{D}), \quad (2.72)$$

$$\mathcal{L}_7(x) = 0, \quad (2.73)$$

$$\mathcal{L}_8(x) = g_8 \bar{\Sigma}_{cj}^\mu \Lambda_c \text{tr}(\bar{D} \tau_j \gamma_\mu \gamma_5 i \overleftrightarrow{\partial}_v \bar{D}) + \text{h.c.}, \quad (2.74)$$

$$\begin{aligned} \mathcal{L}_9(x) + \mathcal{L}_{10}(x) + \mathcal{L}_{11}(x) + \mathcal{L}_{12}(x) = & \bar{\Sigma}_{cj}^\mu \Sigma_{cj}^\nu \text{tr}(\bar{D} (G_9 g_{\mu\nu} + G_{10} i \sigma_{\mu\nu}) i \overleftrightarrow{\partial}_v \bar{D}) \\ & + \bar{\Sigma}_{cj}^\mu \Sigma_{ck}^\nu \text{tr}(\bar{D} \tau_j \tau_k (G_{11} g_{\mu\nu} + G_{12} i \sigma_{\mu\nu}) i \overleftrightarrow{\partial}_v \bar{D}). \end{aligned} \quad (2.75)$$

Here j, k are isovector indices, $\vec{\tau}$ are the Pauli matrices and $\langle 3/2, M | \vec{\epsilon} \lambda \vec{T}^\dagger | 1/2, m \rangle = C(1/2, 1, 3/2; m, \lambda, M)$. Further,

$$G_9 = g_9 + 2g_{11}, \quad G_{10} = g_{10} + 2g_{12}, \quad G_{11} = -g_{11}, \quad G_{12} = -g_{12}. \quad (2.76)$$

Our WT model with SF and HQSS gives the following values for the parameters:

$$\begin{aligned} \hat{g}_1 = 0, \quad \hat{g}_2 = 0, \quad \hat{g}_3 = \sqrt{\frac{3}{2}}, \quad \hat{g}_4 = \sqrt{\frac{1}{6}}, \quad \hat{g}_5 = -1, \quad \hat{g}_6 = \frac{1}{2}, \\ \hat{g}_7 = -\frac{1}{2}, \quad \hat{g}_8 = \frac{1}{2}, \quad \hat{g}_9 = 0, \quad \hat{g}_{10} = 0, \quad \hat{g}_{11} = -\frac{1}{2}, \quad \hat{g}_{12} = -\frac{1}{2}. \end{aligned} \quad (2.77)$$

where we have defined $\hat{g}_i = 4f^2 g_i$.

The vanishing of g_1 and g_2 follows from the OZI rule, which is fulfilled by the model.

III. COUPLED-CHANNELS UNITARIZATION AND SYMMETRY BREAKING

A. Unitarization and renormalization scheme

As previously discussed, the baryon-meson interaction is mediated by the extended WT interaction of Eq. (2.22) that fulfills $SU(6) \times HQSS$ and it is consistent with chiral symmetry in the light sector. The final expression for the potential to be used throughout this work is

$$V_{ij}^{CSIJ} = D_{ij}^{CSIJ} \frac{1}{4f_i f_j} (k_i^0 + k_j^0), \quad (3.1)$$

where k_i^0 and k_j^0 are the CM energies of the incoming and outgoing mesons, respectively, and f_i and f_j are the decay constants of the meson in the i -channel and j -channel.¹⁵ We use the hadron masses and meson decay constants compiled in Table II of Ref. [83]. In particular, $f_{J/\Psi}$ is taken from the width of the $J/\Psi \rightarrow e^-e^+$ decay, that is, $f_{J/\Psi} = 290$ MeV and we set $f_{\eta_c} = f_{J/\Psi}$, as predicted by HQSS and corroborated in the lattice evaluation of Ref. [118]. The D_{ij} are the matrix elements of H'_{WT} , Eq. (2.22), for the various hidden charm $CSIJ$ sectors previously discussed. Those for the strangeless hidden charm $C = 0$ case, for which $H'_{WT} = H_{\text{ex}}$, and that we will discuss in what follows are given in Appendix B.¹⁶

In order to calculate the scattering amplitudes, T_{ij} , we solve the on-shell Bethe-Salpeter equation (BSE), using the matrix V^{CSIJ} as kernel:

$$T^{CSIJ} = (1 - V^{CSIJ} G^{CSIJ})^{-1} V^{CSIJ}, \quad (3.2)$$

where G^{CSIJ} is a diagonal matrix containing the baryon-meson propagator for each channel. Explicitly

$$G_{ii}^{CSIJ}(s) = \frac{(\sqrt{s} + M_i)^2 - m_i^2}{2\sqrt{s}} (\bar{J}_0(\sqrt{s}; M_i, m_i) - \bar{J}_0(\mu^{SI}; M_i, m_i)), \quad (3.3)$$

M_i (m_i) is the mass of the baryon (meson) in the channel i . The loop function \bar{J}_0 can be found in the appendix of [48] (Eq. A9) for the different possible Riemann sheets. The baryon-meson propagator is logarithmically ultraviolet divergent, thus, the loop needed to be renormalized. This has been done by a subtraction point regularization such that

$$G_{ii}^{CSIJ}(s) = 0 \quad \text{at} \quad \sqrt{s} = \mu^{CSI}, \quad (3.4)$$

with $\mu^{CSI} = \sqrt{m_{\text{th}}^2 + M_{\text{th}}^2}$, where m_{th} and M_{th} are, respectively, the masses of the meson and baryon producing the lowest threshold (minimal value of $m_{\text{th}} + M_{\text{th}}$) for each CSI sector, independent of the angular momentum J . This renormalization scheme was first proposed in Refs. [65, 66] and it was successfully used in Refs. [56, 81, 83]. A recent discussion on the regularization method can be found in Ref. [60].

The dynamically-generated baryon resonances appear as poles of the scattering amplitudes on the complex energy \sqrt{s} plane. One has to check both first and second Riemann sheets. The poles of the scattering amplitude on the first Riemann sheet that appear on the real axis below threshold are interpreted as bound states. The poles that are found on the second Riemann sheet below the real axis and above threshold are identified with resonances¹⁷. The mass and

¹⁵ As compared to our previous work of Ref. [83], we have

- approximated $(2\sqrt{s} - M_i - M_j)$, with M_i and M_j the incoming and outgoing baryon masses, by the sum of the CM energies of the incoming and outgoing mesons. In the present case, the non relativistic approximation tends to increase the binding by up to few tens of MeV. This non-relativistic approximation for the baryons is consistent with the treatment for the baryons adopted in the previous section to implement the HQSS constraints, and it makes easier to connect with the effective HQSS Lagrangians introduced in Eqs. (2.57)–(2.66).
- and, also for this latter reason, moved the $\sqrt{(E + M)/(2M)}$ factors included in the potential used in [83] to the definition of the loop function in Eq. (3.3).

¹⁶ For the sake of completeness, and to make possible the determination (see Eq. (2.77)) of the coupling g_7 of the HQSS effective Lagrangian of Eq. (2.63), we also give in the Appendix B the coefficients for the rest of hidden charm sectors with explicit strangeness.

¹⁷ Often we refer to all poles generically as resonances, regardless of their concrete nature, since usually they can decay through other channels not included in the model space.

the width of the state can be found from the position of the pole on the complex energy plane. Close to the pole, the scattering amplitude behaves as

$$T_{ij}^{CSIJ}(s) \approx \frac{g_i e^{i\phi_i} g_j e^{i\phi_j}}{\sqrt{s} - \sqrt{s_R}}. \quad (3.5)$$

The mass M_R and width Γ_R of the resonance result from $\sqrt{s_R} = M_R - i\Gamma_R/2$, while $g_j e^{i\phi_j}$ (modulus and phase) is the coupling of the resonance to the j -channel.

B. Symmetry breaking

As it was already pointed out in the subsection II E, we classify states under the symmetry group $SU(6) \times HQSS$, and consider the breaking of the light SF $SU(6)$ to $SU(3) \times SU_{J_i}(2)$. Subsequently we break the $SU(3)$ light flavor group to $SU(2)$ isospin symmetry group, preserving the $HQSS$, and finally we break the $HQSS$. Thus, we assume exact isospin, total spin and flavor conservation. The symmetry breaking is performed by adiabatic change of hadron masses and meson weak decay constants, as it was previously done in Ref. [83]. At each symmetric point, the hadron masses and meson decay constants are averaged over the corresponding group multiplets. Further, we introduce three parameters, x, x' and x'' that are changed from 0 to 1, to gradually break the symmetry from $SU(6) \times HQSS$ down to $SU(3) \times HQSS$, then to $SU(2) \times HQSS$, and finally down to $SU(2)$ isospin, respectively:

$$\begin{aligned} m(x) &= (1-x) m_{SU(6) \times HQSS} + x m_{SU(3) \times HQSS}, \\ f(x) &= (1-x) f_{SU(6) \times HQSS} + x f_{SU(3) \times HQSS}, \\ m(x') &= (1-x') m_{SU(3) \times HQSS} + x' m_{SU(2) \times HQSS}, \\ f(x') &= (1-x') f_{SU(3) \times HQSS} + x' f_{SU(2) \times HQSS}, \\ m(x'') &= (1-x'') m_{SU(2) \times HQSS} + x'' m_{SU(2)}, \\ f(x'') &= (1-x'') f_{SU(2) \times HQSS} + x'' f_{SU(2)}. \end{aligned} \quad (3.6)$$

In this way we can assign $SU(3)$ and $SU(6)$ representation labels to each found resonance, and also identify the $HQSS$ multiplets. We will show below a diagram (Fig. 3) with the evolution of the hidden charm N and Δ pole positions as the various symmetries are gradually broken.

IV. CHARMLESS AND STRANGELESS HIDDEN CHARM SECTOR: THE N AND Δ STATES

In this work we will only discuss results on hidden charm baryon resonances with total charm $C = 0$ and strangeness $S = 0$. Other sectors with charm different from zero will be studied elsewhere.

In this sector, we find several $I = 1/2$ and $I = 3/2$ states, which correspond to N -like and Δ -like states, respectively (here we use the same notation as in Refs. [74, 75]). All these states have odd parity and different values ($J = 1/2, 3/2$ and $5/2$) of total angular momentum. The list of coupled-channels and the corresponding coefficients D_{ij}^{IJ} can be found in the first six tables of Appendix B.

In this hidden charm sector and in the $SU(6) \times HQSS$ limit, we saw (Eqs. (2.27) and (2.28)) that the group structure of the $HQSS$ -constrained extension of the WT interaction developed in this work consists of two **56_{2,0}** and one **70_{2,0}** representations. One of the **56_{2,0}** multiplets and the **70_{2,0}** one are attractive. Thus, from the decomposition in Eq. (2.29) (see also Table I), we could expect up to a total of ten N -like and seven Δ -like resonances.¹⁸ Because of the breaking of the $SU(6) \times HQSS$ symmetry, due to the use of physical hadron masses and meson decay constants, we only find seven heavy N and five heavy Δ states in the physical Riemann sheets. They have masses around 4 GeV and most of them turn out to be bound. The remaining missing states show up in unphysical Riemann sheets. The evolution of all states as we gradually break the symmetry from $SU(6) \times HQSS$ down to $SU(3) \times HQSS$, then to $SU(2) \times HQSS$, and finally down to $SU(2)$ isospin, is depicted in Fig. 3. Thanks to this latter study, we could assign $SU(6) \times HQSS$ and $SU(3) \times HQSS$ labels to each of the predicted resonances, which are all of them collected in Tables II and IV, and could also identify two $HQSS$ multiplets in each isospin sector.

¹⁸ Those lie in the $SU(3)$ octets and decuplets irreps, respectively, contained in the attractive **56_{2,0}** and **70_{2,0}** multiplets.

A. N states ($C = 0, S = 0, I = 1/2$)

As mentioned above, the model predicts the existence of seven heavy nucleon resonances: three states with the spin-parity $J^P = \frac{1}{2}^-$, also three states with $\frac{3}{2}^-$ sectors, and one state with $J^P = \frac{5}{2}^-$. Their masses, widths and couplings to the different channels are compiled in Table II.

- $J = 1/2$: In this sector, there are seven coupled channels, with the following threshold energies (in MeV):

$$\begin{array}{ccccccc} N\eta_c & NJ/\psi & \Lambda_c \bar{D} & \Lambda_c \bar{D}^* & \Sigma_c \bar{D} & \Sigma_c \bar{D}^* & \Sigma_c^* \bar{D}^* \\ 3918.6 & 4035.8 & 4153.7 & 4294.8 & 4320.8 & 4461.9 & 4526.3 \end{array}$$

- $J = 3/2$: In this sector, there are five coupled channels, with the following threshold energies:

$$\begin{array}{ccccc} NJ/\psi & \Lambda_c \bar{D}^* & \Sigma_c^* \bar{D} & \Sigma_c \bar{D}^* & \Sigma_c^* \bar{D}^* \\ 4035.8 & 4294.8 & 4385.2 & 4461.9 & 4526.3 \end{array}$$

- $J = 5/2$: In this sector there is only one channel, $\Sigma_c^* \bar{D}^*$, with threshold equal to 4526.3 MeV.

From the group decomposition of the $SU(6) \times HQSS$ representations, we could expect up to a maximum of five states with spin $J = 1/2$ (see Table I): one state from each of the two $J = 1/2$ octets encoded in the attractive $\mathbf{56}_{2,0}$ representation, and three states corresponding to the each of the $\mathbf{8}_2$ octets that appear in the reduction of the $\mathbf{70}_{2,0}$ representation [Eq. (2.29)]. However, the two poles related to the $\mathbf{56}_{2,0}$ representation appear in an unphysical Riemann sheet, at the physical point (i.e., at the point of the evolution when the hadron masses and meson decay constants attain their physical values). As it can be seen from Fig. 3, these poles disappear from the physical sheet when we pass from the $SU(3) \times HQSS$ limit to the $SU(2) \times HQSS$ one. Indeed, we could observe how the $(\mathbf{8}_2)_{2,0} \subset (\mathbf{56}_2)_{2,0}$ pole almost coincides with the threshold value of the degenerated $N\eta_c$ and NJ/ψ channels in the first steps of this evolution until it finally disappears. On the other hand, the $(\mathbf{8}_2)_{2,0} \subset (\mathbf{56}_2)_{2,0}$ pole also gives rise to an octet of $J = 3/2$ states (see Eq. (2.29)), which is also lost at the physical point. Thus, for $J = 3/2$ we are also left only with the three baryon resonances stemming from the $\mathbf{70}_{2,0}$ representation, one from $(\mathbf{8}_2)_{2,0}$, and two from $(\mathbf{8}_4)_{2,0}$. The $J = 5/2$ state is originated also from this latter multiplet.

From the above discussion, it is clear that the N -like resonances found in this work, and collected in Table II, form two HQSS multiplets. In the first one the light degrees of freedom have quantum numbers $(\mathbf{8}_2)_{2,0} \subset (\mathbf{70}_2)_{2,0}$. This multiplet is formed by the three first resonances of the table (two with spin 1/2 and third one with spin 3/2) that correspond to the blue states in Fig. 3. They only differ in how the light sector spin is coupled to the spin of the $c\bar{c}$ pair. The second HQSS multiplet corresponds to $(\mathbf{8}_4)_{2,0} \subset (\mathbf{70}_2)_{2,0}$ quantum numbers for the light sector, and it consists of the four remaining states in Table II (displayed in green in Fig. 3) one with spin 1/2, two with spin 3/2, and another one with spin 5/2.

The members of each HQSS multiplet are nearly degenerate, but not totally because we also break the HQSS by the use of physical hadron masses.

A word of caution is needed here. The mass of the $J = 5/2$ resonance is around 4027.2 MeV. In this sector there is only one channel ($\Sigma_c^* \bar{D}^*$, with threshold equal to 4526.3 MeV), thus this state is around five hundred MeV bound. We expect our model to work well close to threshold, and therefore, in this case, interaction mechanisms neglected here and involving higher partial waves could be relevant for determining the actual properties of this resonance.

There exist previous works on hidden-charm odd-parity nucleon states, also named crypto-exotic hadronic states. These studies can be divided in two types. Namely, those based on a constituent quark description of the resonances, and those where they are described as baryon-meson bound molecules or resonating states. Some of the predictions of these other models are compiled in Table III.

The baryon-meson coupled-channel calculations by Hofmann and Lutz for $J^P = 1/2^-$ in Ref. [65] and for $J^P = 3/2^-$ in Ref. [66] rely on a model of zero-range t -channel exchange of light vector mesons, based on chiral and large N_C considerations, and supplemented with $SU(4)$ input in some vertices. This model is used as the driving interaction of pseudo-scalar mesons with the $J^P = 1/2^+, 3/2^+$ baryon ground states. After solving the BSE using a renormalization scheme similar to that proposed here, some $1/2^-, 3/2^-$ -resonances were dynamically generated. Vector mesons in the coupled-channel space were omitted in those early studies, thus channels like $\Sigma_c \bar{D}^*$ or $\Lambda_c \bar{D}^*$ were not considered.

More recently baryon-meson calculations using a hidden-gauge model have been carried out in Refs. [74–76]. These works consider $1/2^+$ baryons interacting with pseudoscalar mesons and dynamically generate $J^P = 1/2^-$ hidden-charm nucleon resonances as poles in the T -matrix. Yet, the interaction of vector mesons with $1/2^+$ baryons ($VB \rightarrow VB$)

SU(6) \times HQSS irrep	SU(3) \times HQSS irrep	M_R [MeV]	Γ_R [MeV]	Couplings to main channels	J
70_{2,0}	(8₂)_{2,0}	3918.3	0.0	$g_{N\eta_c} = 0.5, g_{NJ/\psi} = 0.6, g_{\Lambda_c \bar{D}} = 3.1, g_{\Lambda_c \bar{D}^*} = 0.5,$ $g_{\Sigma_c \bar{D}} = 0.2, g_{\Sigma_c \bar{D}^*} = 2.6, g_{\Sigma_c^* \bar{D}^*} = 2.6$	1/2
70_{2,0}	(8₂)_{2,0}	3926.0	0.1	$g_{N\eta_c} = 0.2$, $g_{NJ/\psi} = 0.04, g_{\Lambda_c \bar{D}} = 0.4, g_{\Lambda_c \bar{D}^*} = 3.0,$ $g_{\Sigma_c \bar{D}} = 4.2, g_{\Sigma_c \bar{D}^*} = 0.2, g_{\Sigma_c^* \bar{D}^*} = 0.7$	1/2
70_{2,0}	(8₂)_{2,0}	3946.1	0.	$g_{NJ/\psi} = 0.2, g_{\Lambda_c \bar{D}^*} = 3.4, g_{\Sigma_c^* \bar{D}} = 3.6, g_{\Sigma_c \bar{D}^*} = 1.1,$ $g_{\Sigma_c^* \bar{D}^*} = 1.5$	3/2
70_{2,0}	(8₄)_{2,0}	3974.3	2.8	$g_{N\eta_c} = 0.5$, $g_{NJ/\psi} \sim 0.05, g_{\Lambda_c \bar{D}} = 0.4, g_{\Lambda_c \bar{D}^*} = 2.2,$ $g_{\Sigma_c \bar{D}} = 2.1, g_{\Sigma_c \bar{D}^*} = 3.4, g_{\Sigma_c^* \bar{D}^*} = 3.1$	1/2
70_{2,0}	(8₄)_{2,0}	3986.5	0.	$g_{NJ/\psi} = 0.2, g_{\Lambda_c \bar{D}^*} = 1.0, g_{\Sigma_c^* \bar{D}} = 2.7, g_{\Sigma_c \bar{D}^*} = 4.3,$ $g_{\Sigma_c^* \bar{D}^*} = 1.8$	3/2
70_{2,0}	(8₄)_{2,0}	4005.8	0.	$g_{NJ/\psi} = 0.3, g_{\Lambda_c \bar{D}^*} = 1.0, g_{\Sigma_c^* \bar{D}} = 1.6, g_{\Sigma_c \bar{D}^*} = 3.2,$ $g_{\Sigma_c^* \bar{D}^*} = 4.2$	3/2
70_{2,0}	(8₄)_{2,0}	4027.1	0.	$g_{\Sigma_c^* \bar{D}^*} = 5.6$	5/2

TABLE II: Odd parity hidden charm N ($J = 1/2$, $J = 3/2$ and $J = 5/2$) resonances found in this work. The first two columns contain the SU(6) \times HQSS and SU(3) \times HQSS quantum numbers of each state, while M_R and Γ_R stand for its mass and width (in MeV). The largest couplings of each pole, ordered by their threshold energies, are collected in the next column. In boldface, we highlight the channels which are open for decay. Finally, the spin of the state is given in the last column. Resonances with equal SU(6) \times HQSS and SU(3) \times HQSS labels form HQSS multiplets, and they are collected in consecutive rows.

is also taken into account in [74–76], which leads to additional and degenerate $J^P = 1/2^-$ and $3/2^-$ hidden-charm nucleons. However, the $J = 3/2^+$ baryons are not included at all, and thus some channels like $\Sigma_c^* \bar{D}^*$ are excluded.

The main difference among our scheme and the hidden-gauge models is the definition of the coupled-channels space. We consider simultaneously pseudoscalar meson–baryon (PB) and vector meson–baryon (VB) channels, with $J^P = 1/2^+$ and $3/2^+$ baryons. However in the approaches of Refs. [74–76] all interaction terms of the type $PB \rightarrow VB$ are neglected. Furthermore, channels with $J^P = 3/2^+$ baryons are not considered either. The potential used in [74–76] for the $PB \rightarrow PB$ transitions, with $J^P = 1/2^+$ baryons, is similar to that derived here. However, there exist important differences in all transitions involving vector mesons. When restricting our model to the $PB \rightarrow PB$ sector, we still do not obtain the same results as in Refs. [74–76]. This is mainly due to i) the use of a different renormalization scheme and, ii) the presence in these latter works of a suppression factor in those transitions that involve a t -channel exchange of a heavy charm vector meson.

However, when we use our full space, the inclusion of a similar suppression factor in our HQSS kernel is not quantitatively relevant for the dynamical generation of the resonances. Note that HQSS does not require the presence of such suppression factor. In summary, when we compare our approach with the other molecular-type ones, we observe in our model a rich structure of resonances due to the many channels cooperating to create them. Our states are much more lighter than those predicted in Refs. [74–76], though significantly less bound than the crypto-exotic baryons reported in Refs. [65, 66].

Finally, we will pay attention to the recent work of Ref. [119]. There a constituent quark model is used to describe isospin $I = 1/2$ baryons with $uudc\bar{c}$ quark content. The mass spectra is evaluated with three types of hyperfine interactions: color-magnetic interaction (CM) based on one-gluon exchange, chiral interaction (FS) based on meson exchange, and instanton-induced interaction (INST) based on the non-perturbative QCD vacuum structure. The FS (CM) model predicts the lowest (highest) mass for each state. Results for the FS and CM models are displayed in Table III. In all cases, the mass predicted by the INST model (not displayed in the table) lies between the values predicted by the other two models. Our results are closer to those predicted by the FS model, specially for the lowest lying states.

B. Δ states ($C = 0, S = 0, I = 3/2$)

The model predicts in this sector the existence of five heavy resonances (bound states; all of them appear below threshold): three with spin-parity $J^P = \frac{1}{2}^-$ and another two with $J^P = \frac{3}{2}^-$. Their masses, widths and couplings to the different channels are compiled in Table IV.

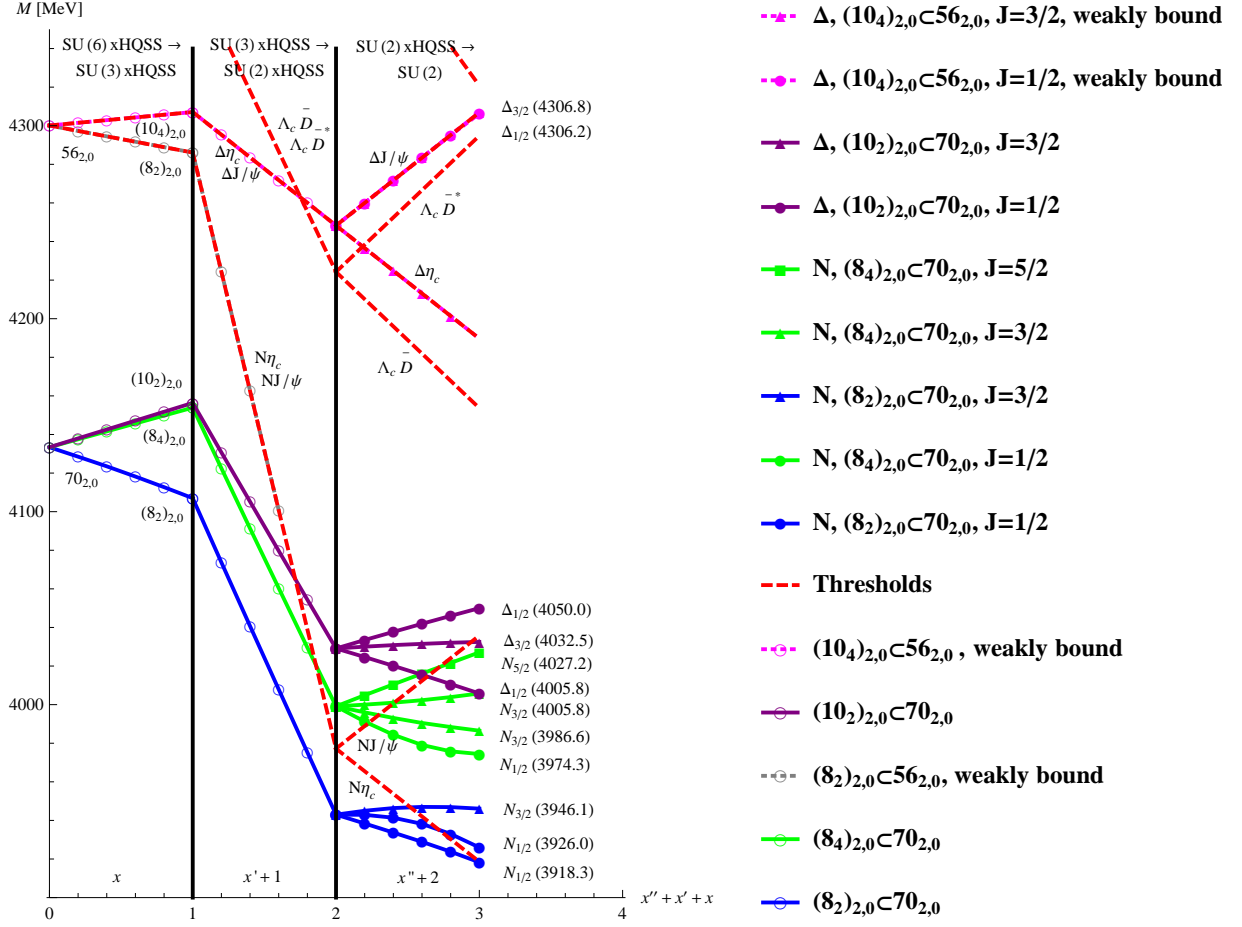


FIG. 3: Evolution of the poles as symmetries, starting from $SU(6) \times HQSS$, are sequentially broken to reach the isospin symmetric final crypto-exotic N and Δ odd-parity resonances. The meanings of x , x' and x'' can be found in (3.6). The lower index of the final states stands for the spin J of the corresponding resonance. The thresholds (red dashed lines) are marked together with the respective baryon-meson channel. The $SU(6) \times HQSS$ labels $70_{2,0}$ and $56_{2,0}$, and the $SU(3) \times HQSS$ labels $(8_2)_{2,0}$, $(8_4)_{2,0}$, $(10_2)_{2,0}$, $(10_4)_{2,0}$ are also shown at the corresponding symmetric points.

- $J = 1/2$: In this sector, there are four coupled channels, with the following threshold energies (in MeV):

$$\begin{array}{cccc} \Delta J/\psi & \Sigma_c \bar{D} & \Sigma_c \bar{D}^* & \Sigma_c^* \bar{D}^* \\ 4306.9 & 4320.8 & 4461.9 & 4526.3 \end{array}$$

- $J = 3/2$: In this sector, there are five coupled channels, with the following threshold energies:

$$\begin{array}{ccccc} \Delta \eta_c & \Delta J/\psi & \Sigma_c^* \bar{D} & \Sigma_c \bar{D}^* & \Sigma_c^* \bar{D}^* \\ 4189.7 & 4306.9 & 4385.2 & 4461.9 & 4526.3 \end{array}$$

- $J = 5/2$: In this sector there are only two channels, with the following threshold energies:

$$\begin{array}{cc} \Delta J/\psi & \Sigma_c^* \bar{D}^* \\ 4306.9 & 4526.3 \end{array}$$

Ref.	Model	$N(1/2^-)$						$N(3/2^-)$					$N(5/2^-)$			
		M_R [MeV]	g to main-channels					M_R [MeV]	g to main-channels				M_R [MeV]	g $\Sigma_c^* \bar{D}^*$		
		$\Lambda_c \bar{D}$	$\Lambda_c \bar{D}^*$	$\Sigma_c \bar{D}$	$\Sigma_c \bar{D}^*$	$\Sigma_c^* \bar{D}^*$		$\Lambda_c \bar{D}^*$	$\Sigma_c^* \bar{D}$	$\Sigma_c \bar{D}^*$	$\Sigma_c^* \bar{D}^*$					
This work	$(\mathbf{8_2})_{2,0} \subset (\mathbf{70_2})_{2,0}$	3918	3.1	0.5	0.2	2.6	2.6	3946	3.4	3.6	1.1	1.5				
		3926	0.4	3.0	4.2	0.2	0.7									
	$(\mathbf{8_4})_{2,0} \subset (\mathbf{70_2})_{2,0}$	3974	0.4	2.2	2.1	3.4	3.1	3987	1.0	2.7	4.3	1.8	4027	5.6		
							4006	1.0	1.6	3.2	4.2					
[65][66]	zero-range vector exchange	3520			5.3			3430			5.6					
[75]	hidden-gauge	4265	0.1		3.0			4415	0.1		2.8					
		4415		0.1		2.8										
[76]	hidden-gauge	4315	X		X			4454	X		X					
		4454		X		X										
[119]	quark model $uudc\bar{c}$	FS-CM						FS-CM								
		3933-4267														
		4013-4363						4013-4389								
		4119-4377						4119-4445								
		4136-4471						4136-4476								
		4156-4541						4236-4526								

TABLE III: Comparison of the whole spectrum of hidden-charm nucleons (or crypto-exotic nucleons) with odd-parity and angular momentum $L = 0$ predicted by our model with some results from previous models. In all cases, masses and couplings (g) to the dominant channels (when available) are shown in sequential rows. In the hidden gauge model of Ref. [76], the numerical values of the couplings are not given. In this case, we indicate with a symbol X the elements of the coupled channel space used to generate each resonance. On the other hand, in the case of the predictions of this work, in the column “Model” we give the HQSS multiplet. Besides, we have also omitted the small couplings to the $N\eta_c$ and NJ/ψ channels that can be seen in Table II.

We obtain three $\Delta(J = 1/2)$ states as expected from the group decomposition of the $SU(6) \times \text{HQSS}$ representations (see Table I): one state from each of the two $J = 1/2$ decuplets encoded in the attractive $\mathbf{70}_{2,0}$ representation, and a further state corresponding to the $J = 1/2$ decuplet that appears in the reduction of the $\mathbf{56}_{2,0}$ representation [Eq. (2.29)]. The evolution of the corresponding poles is shown in Fig. 3.

The pole that corresponds to $(\mathbf{10}_4)_{2,0} \subset \mathbf{56}_{2,0}$ (light magenta circles in Fig. 3) has a mass quite close to the $\Delta\eta_c$ and $\Delta J/\psi$ degenerated thresholds, between the $SU(6) \times \text{HQSS}$ and the $SU(2) \times \text{HQSS}$ symmetric points. Later, while moving to the $SU(2)$ isospin symmetric point, the spin $1/2$ Δ resonance keeps having a mass close to the $\Delta J/\psi$ threshold, and ends up with a final mass of 4306.2 MeV (the $\Delta J/\psi$ threshold is at 4306.9 MeV). However, the spin $5/2$ and the two spin $3/2$ states, that are also originated from this $(\mathbf{10}_4)_{2,0} \subset \mathbf{56}_{2,0}$ pole, essentially disappear. One of the $J = 3/2$ states still shows up as a cusp very close to the $\Delta J/\psi$ threshold, and it has been included in the table. The second state with spin $3/2$ (light magenta triangles in Fig. 3) and the spin $5/2$ one appear as small unnoticeable peaks right at the $\Delta\eta_c$ and $\Delta J/\Psi$ thresholds, respectively.

From the discussion above, the $(\mathbf{10}_4)_{2,0} \subset \mathbf{56}_{2,0}$ HQSS multiplet could be incomplete.

However the three Δ states (dark magenta circles for the two $J^P = 1/2^-$ states and dark magenta triangles for the $J^P = 3/2^-$ resonance in Fig. 3) that stem from the $(\mathbf{10}_2)_{2,0} \subset \mathbf{70}_{2,0}$ configuration of the light degrees of freedom turn out to be quite bound. Indeed, we find binding energies of at least 250 (150) MeV in the spin $1/2$ ($3/2$) sector. These three states, nearly degenerate, form a clear HQSS multiplet.

The models based on vector meson exchange, naturally predict a suppression factor in the baryon-meson amplitudes involving exchange of charm, from the propagator of the exchanged heavy vector meson. In the heavy quark limit, the suppression factor is of the order of $1/m_H$.¹⁹ Therefore, in that limit, one expects a quenching of order M_V/M_{D^*} for the charm exchanging amplitudes of those models. (Of course, the true factor for large but finite physical heavy

¹⁹ The boson propagator is approximately $1/(2M_H(E_H - M_H))$, with M_H the mass of the heavy vector meson and E_H its energy, and $E_H - M_H$ is $O(1)$ in the heavy quark limit.

SU(6) \times HQSS irrep	SU(3) \times HQSS irrep	M_R	Γ_R	Couplings to main channels	J
70 _{2,0}	(10 ₂) _{2,0}	4005.8	0.	$g_{\Delta J/\psi} = 0.3, g_{\Sigma_c \bar{D}} = 2.7, g_{\Sigma_c \bar{D}^*} = 4.4, g_{\Sigma_c^* \bar{D}^*} = 1.2$	1/2
70 _{2,0}	(10 ₂) _{2,0}	4032.5	0.	$g_{\Delta \eta_c} = 0.2, g_{\Delta J/\psi} = 0.1, g_{\Sigma_c^* \bar{D}} = 2.9, g_{\Sigma_c \bar{D}^*} = 1.8$ $g_{\Sigma_c^* \bar{D}^*} = 4.1$	3/2
70 _{2,0}	(10 ₂) _{2,0}	4050.0	0.	$g_{\Delta J/\psi} = 0.2, g_{\Sigma_c \bar{D}} = 0.8, g_{\Sigma_c \bar{D}^*} = 1.9, g_{\Sigma_c^* \bar{D}^*} = 5.1$	1/2
56 _{2,0}	(10 ₄) _{2,0}	4306.2	0. (cusp)	$g_{\Delta J/\psi} = 1.3, g_{\Sigma_c \bar{D}} = 0.3, g_{\Sigma_c \bar{D}^*} = 0.3, g_{\Sigma_c^* \bar{D}^*} = 0.3$	1/2
56 _{2,0}	(10 ₄) _{2,0}	4306.8	0. (cusp)	$g_{\Delta \eta_c} \sim 0.1, g_{\Delta J/\psi} = 0.8, g_{\Sigma_c^* \bar{D}} = 0.2, g_{\Sigma_c \bar{D}^*} = 0.2,$ $g_{\Sigma_c^* \bar{D}^*} = 0.1$	3/2

TABLE IV: As in Table II, for the Δ ($J = 1/2, J = 3/2$) resonances with hidden charm content.

hadron masses needs not exactly coincide with this heavy quark limit estimate.) Our model is not directly based on exchange of vector mesons. Nevertheless, as commented above, we have verified that adding such suppression by hand in the charm exchanging amplitudes does not have an impact on our results. Even a factor $(M_V/M_{D^*})^2$, proposed in the literature [68] has a very small effect in the position of the resonances we find. Presumably, this is due to the fact that the relevant channels have a small coupling. An exception comes from the two very weakly bound Δ resonances from the **56**_{2,0} irrep, which disappear due to the suppression of their dominant channel $\Delta J/\psi$.

V. CONCLUSIONS

In the present work we develop a model for the interaction of lowest-lying $1/2^+$ and $3/2^+$ baryons with 0^- and 1^- mesons, including light and heavy flavors. The interaction is of zero range and it is modeled as a suitable extension of the Weinberg-Tomozawa term to include, besides chiral symmetry, spin-flavor symmetry in the light sector and heavy quark spin symmetry. These symmetries are only broken in our model to the extent that they are broken at level of the physical masses and meson decay constants. The OZI rule is also automatically implemented. Our extended WT model, Eq. (2.22), contains no adjustable parameters, although some ambiguity is present through the choice of renormalization prescription, as in all other hadronic molecular approaches. The model has been applied previously to the light sector and to charm or bottom sectors with a single heavy quark. Here we show that it admits a natural realization in sectors with hidden charm in such a way that HQSS is preserved. In particular, the spin of c quarks and the spin of \bar{c} antiquarks are separately conserved.

We have carried out a detailed analysis of the hidden charm sectors (i.e., with $c\bar{c}$ pairs) with $C = 0, 1, 2, 3$ and their breaking as the symmetry is lifted from SU(6) \times HQSS to SU(3) \times HQSS (and then to SU(2) \times HQSS and SU(2) of isospin). This allows to count the expected number of bound states or resonances, and to classify them into multiplets corresponding to the various symmetries. Taking the eigenvalues λ 's as undetermined (free) parameters, the results of Eqs. (2.30), (2.35), (2.38) and (2.42), for the $C = 0$, $C = 1$, $C = 2$ and $C = 3$ hidden charm sectors respectively, are general. Indeed, these equations fix the most general structure of eigenvalues that can be deduced from SU(3) \times HQSS. The rest of undetermined parameters, not fixed by this latter symmetry, accounts for non-diagonal transitions between multiplets with the same SU(3) \times SU(J_ℓ)(2) SF quantum numbers for the light degrees of freedom. Further, we have translated this general discussion of the group structure allowed by SU(3) \times HQSS into Lagrangian form, for the charmless hidden-charm sector. This makes the HQSS of the model explicit and it allows to compare with other models in the literature. Finally, we have found the couplings of the HQSS effective Lagrangians of Eqs. (2.57)–(2.66) for the particular case of our extended WT model. This constitutes an additional check of its compatibility with HQSS.

We have analyzed the charmless and strangeless sector, where we have dynamically generated several N and Δ states. Actually, we predict the existence of seven N -like and five Δ -like states with masses around 4 GeV, most of them as bound states. These states form heavy-quark spin multiplets, which are almost degenerate in mass. The N states form two HQSS multiplets. The lowest one has the light quark flavor-spin content coupled to **8**₂. Since the $c\bar{c}$ pair can couple to spin $S_{c\bar{c}} = 0, 1$, this HQSS multiplet consists of three nucleon states with $J = 1/2, 1/2$, and $3/2$, and masses around 3930 MeV. On the other hand, the highest HQSS nucleon-like multiplet contains four resonances with $J = 1/2, 3/2, 3/2$ and $5/2$, and masses around 4000 MeV. In this case, these states are originated from the **8**₄ SF light configuration. These two SU(3) \times HQSS multiplets arise from the **70**-plet of SU(6) \times HQSS. There are no N physical states coming from the **56**-plet. With regards to Δ states, we find two multiples with very different

average masses, because in this case they are originated from different $SU(6) \times HQSS$ representations. The Δ multiplet coming from the $(\mathbf{10}_2)_{2,0} \subset \mathbf{70}_{2,0}$ irrep is formed by 3 states ($J = 1/2, 1/2, 3/2$) with an average mass of 4035 MeV. Besides, we find only two ($J = 1/2, 3/2$) Δ resonances at the physical point out of the four states originated from the $(\mathbf{10}_4)_{2,0} \subset \mathbf{56}_{2,0}$ in the $SU(6)$ limit. These two states are nearly degenerate, with a mass of 4306 MeV.

When we compare our approach with the other molecular-type ones, we observe in our model a rich structure of resonances due to the many channels cooperating to create them. Our states are much more lighter than those predicted in the hidden-gauge scheme [74–76], though significantly less bound than the crypto-exotic baryons reported in the zero range vector meson exchange model of Refs. [65, 66]. Moreover, we have presented the first prediction for exotic hidden-charm Δ -like resonances within a molecular baryon-meson scheme.

In comparison with the quark model of Ref. [119], we find that our results are closer to those predicted by the FS hyperfine interaction discussed in Ref. [119], specially for the lowest lying states.

The predicted new resonances definitely cannot be accommodated by quark models with three constituent quarks and they might be looked for in the forthcoming PANDA experiment at the future FAIR facility.

Acknowledgments

This research was supported by Spanish DGI and FEDER funds, under contracts FIS2011-28853-C02-02, FIS2011-24149, FPA2010-16963 and the Spanish Consolider-Ingenio 2010 Programme CPAN (CSD2007-00042), by Junta de Andalucía grant FQM-225, by Generalitat Valenciana under contract PROMETEO/2009/0090 and by the EU HadronPhysics2 project, grant agreement n. 227431. O.R. wishes to acknowledge support from the Rosalind Franklin Fellowship. L.T. acknowledges support from Ramon y Cajal Research Programme, and from FP7-PEOPLE-2011-CIG under contract PCIG09-GA-2011-291679.

Appendix A: Spin-flavor states

In this appendix we give details regarding the construction of the tensors M^A_B and B^{ABC} , the $SU(3)$ multiplets Σ^a_b , \bar{D}^a , etc, and the computation of the matrix elements of the interaction.

The wave-functions in spin-flavor space of the basic mesons and baryons are constructed in terms of bosonic quark and antiquark operators with spin and flavor labels, namely, $Q_{f\uparrow}^\dagger, Q_{f\downarrow}^\dagger, Q_{\bar{f}\uparrow}^\dagger, Q_{\bar{f}\downarrow}^\dagger$, $f = u, d, s, c$. The concrete wave-functions are those given in the Appendix A of [81] with the following modification: a minus sign is to be applied to all $1/2^+$ baryons, to all 0^- mesons except η , η' and η_c , and to ϕ , ω and J/ψ (denoted ψ in [81]). No change of sign is to be applied to $3/2^+$ baryons, nor to η , η' and η_c , nor to 1^- mesons (except ϕ , ω and J/ψ).

The states just defined are standard with respect to the flavor and spin-flavor groups conventions of [111]. In particular they are $SU(2)_J$, $SU(2)_I$ standard and follow the convention of [116] for flavor $SU(3)$ and $SU(4)$. The only exceptions come from the neutral mesons for which we use ideal mixing. In terms of these, the standard states of [111] are given by:

$$|\eta'\rangle_{\text{stan}} = |\eta'\rangle \quad (SU(3)), \quad (A1)$$

$$|\eta'\rangle_{\text{stan}} = \sqrt{\frac{3}{4}}|\eta'\rangle + \frac{1}{2}|\eta_c\rangle \quad (SU(4)), \quad (A2)$$

$$|\eta_c\rangle_{\text{stan}} = -\frac{1}{2}|\eta'\rangle + \sqrt{\frac{3}{4}}|\eta_c\rangle \quad (SU(4)), \quad (A3)$$

$$|\omega_8\rangle = \sqrt{\frac{1}{3}}|\omega\rangle + \sqrt{\frac{2}{3}}|\phi\rangle \quad (SU(3) \text{ and } SU(4)), \quad (A4)$$

$$|\omega_1\rangle = \sqrt{\frac{2}{3}}|\omega\rangle - \sqrt{\frac{1}{3}}|\phi\rangle \quad (SU(3)), \quad (A5)$$

$$|\omega_1\rangle = \sqrt{\frac{1}{2}}|\omega\rangle - \frac{1}{2}|\phi\rangle + \frac{1}{2}|J/\psi\rangle \quad (SU(4)), \quad (A6)$$

$$|\psi\rangle = -\sqrt{\frac{1}{6}}|\omega\rangle + \sqrt{\frac{1}{12}}|\phi\rangle + \sqrt{\frac{3}{4}}|J/\psi\rangle \quad (SU(4)). \quad (A7)$$

In these formulas, the right-hand sides contain the physical (or rather ideal mixing) neutral mesons that we use in this work. Their wave-functions are constructed as indicated above (i.e., from those in [81]). The left-hand sides contain

the standard or mathematical states used in [111]. They have good quantum numbers with respect to SU(6) or SU(8) (and their corresponding chain of subgroups).²⁰

In order to construct the tensors M^A_B and B^{ABC} , $M^{\dagger A}_B$ and B^{\dagger}_{ABC} , with good transformations properties, the following procedure is used: For all flavors $f = u, d, s, c$, and for the various creation operators $Q_{f\uparrow}^\dagger$, $Q_{f\downarrow}^\dagger$, $Q_{\bar{f}\uparrow}^\dagger$, and $Q_{\bar{f}\downarrow}^\dagger$, appearing in the wave-functions of the hadrons, the following replacements are to be applied:

$$Q_{f\uparrow}^\dagger \rightarrow +Q_{f1}^\dagger, \quad Q_{f\downarrow}^\dagger \rightarrow +Q_{f2}^\dagger, \quad Q_{\bar{f}\uparrow}^\dagger \rightarrow -\bar{Q}^{\dagger f2}, \quad Q_{\bar{f}\downarrow}^\dagger \rightarrow +Q_{\bar{f}1}^\dagger \quad (\text{A8})$$

Note i) the minus sign in $Q_{\bar{f}\uparrow}^\dagger$, and ii) for quarks, the labels 1 and 2 correspond to spin up and down, respectively, but for antiquarks they correspond to spin down and up, respectively.

After the replacement, there are only operators Q_A^\dagger , and $\bar{Q}^{\dagger A}$ for creation (and Q^A , and \bar{Q}_A for annihilation), carrying any of the eight labels $A = u1, d1, s1, c1, u2, d2, s2, c2$. These operators transform under SU(8) in the way indicated in Eq. (2.17).

The meson matrix is then obtained by replacing $\bar{Q}^{\dagger A}Q_B^\dagger$ with $M^{\dagger A}_B$ and expressing it in terms of meson operators by inverting the wave-function equations. Similarly, for the baryons, $Q_A^\dagger Q_B^\dagger Q_C^\dagger$ is replaced with B^{\dagger}_{ABC} and then expressed in terms of baryon operators. The fields $\Phi^A_B(x)$ and $\mathcal{B}^{ABC}(x)$ of Section II B are constructed in the usual way from these annihilation and creation operators.

The SU(3) multiplets introduced in Section II F are obtained as follows.

$$\Delta^{abc} = B^{(as_1, bs_2, cs_3)_{3/2}} \quad (\text{A9})$$

Here $A = as_1$, $B = bs_2$, $C = cs_3$, with $a, b, c \in \{u, d, s\}$, $s_1, s_2, s_3 \in \{1, 2\}$, and the notation $(ABC)_{3/2}$ indicates that the spin part is coupled to $J = 3/2$ with $1 = \uparrow$ and $2 = \downarrow$. Besides we refer here to the (annihilation) operator; the field $\Delta_\mu^{abc}(x)$ is constructed out of it.

$$\Sigma^a_b = \sqrt{\frac{1}{6}} \epsilon_{bcd} B^{(as_1(cs_2, ds_3)_0)_{1/2}}, \quad (\text{A10})$$

$$\Sigma_c^{ab} = B^{((as_1, bs_2)_1 cs_3)_{1/2}}, \quad (\text{A11})$$

$$\Sigma_c^{*ab} = B^{((as_1, bs_2)_1 cs_3)_{3/2}}, \quad (\text{A12})$$

$$\Xi_{ca} = \frac{1}{2} \epsilon_{abc} B^{((bs_1, cs_2)_0 cs_3)_{1/2}}, \quad (\text{A13})$$

For the mesons

$$\bar{D}^a = M^{(as_1 cs_2)_0}, \quad (\text{A14})$$

$$\bar{D}^{*a} = -M^{(as_1 cs_2)_1}, \quad (\text{A15})$$

$$\eta_c = M^{(cs_1 cs_2)_0}, \quad (\text{A16})$$

$$J/\psi = -M^{(cs_1 cs_2)_1}. \quad (\text{A17})$$

Recalling that $\bar{Q}_{f1} = Q_{\bar{f}\downarrow}$ and $\bar{Q}_{f2} = -Q_{\bar{f}\uparrow}$, it follows that $M^{(as_1 bs_2)_0} = (M^{a1}_{b1} + M^{a2}_{b2})/\sqrt{2}$, while $M^{(as_1 bs_2)_1}$ equals $-M^{a1}_{b2}$, $(M^{a1}_{b1} - M^{a2}_{b2})/\sqrt{2}$ and M^{a2}_{b1} , for $J_3 = +1, 0, -1$, respectively.

Finally, we remark that we systematically take the coupling of baryon and meson in the order $|\text{baryon}\rangle \otimes |\text{meson}\rangle$, rather than $|\text{meson}\rangle \otimes |\text{baryon}\rangle$.

Appendix B: Baryon-meson matrix elements

The coefficients D_{ij} , appearing in Eq. (3.1), for the charmless ($C = 0$) and strangeless ($S = 0$) sector are compiled in this Appendix (Tables V, VI, VII, VIII, IX and X). In addition, we also provide here the corresponding coefficients

²⁰ Note that $|\psi\rangle$ of [81] corresponds to $-|J/\psi\rangle$ here, not to $|\psi\rangle$ of [111] and of Eq. (A7).

for the $C = 0$ and $S \neq 0$ sectors (Tables XI, XII, XIII, XIV, XV, XVI XVII, XVIII, XIX, XX, XXI, XXII).

-
- [1] B. Aubert *et al.* [BABAR Collaboration], Phys. Rev. Lett. **90**, 242001 (2003).
 - [2] R. A. Briere *et al.* [CLEO Collaboration], Phys. Rev. D **74**, 031106 (2006).
 - [3] P. Krokovny *et al.* [Belle Collaboration], Phys. Rev. Lett. **91**, 262002 (2003).
 - [4] K. Abe *et al.* [Belle Collaboration], Phys. Rev. Lett. **92**, 012002 (2004).
 - [5] S. K. Choi *et al.* [Belle Collaboration], Phys. Rev. Lett. **91**, 262001 (2003).
 - [6] D. E. Acosta *et al.* [CDF II Collaboration], Phys. Rev. Lett. **93**, 072001 (2004).
 - [7] V. M. Abazov *et al.* [D0 Collaboration], Phys. Rev. Lett. **93**, 162002 (2004).
 - [8] B. Aubert *et al.* [BABAR Collaboration], Phys. Rev. D **71**, 071103 (2005).
 - [9] K. Abe *et al.* [Belle Collaboration], Phys. Rev. Lett. **98**, 082001 (2007).
 - [10] P. Pakhlov *et al.* [Belle Collaboration], Phys. Rev. Lett. **100**, 202001 (2008).
 - [11] K. Abe *et al.* [Belle Collaboration], Phys. Rev. Lett. **94**, 182002 (2005).
 - [12] B. Aubert *et al.* [BaBar Collaboration], Phys. Rev. Lett. **101**, 082001 (2008).
 - [13] S. Uehara *et al.* [Belle Collaboration], Phys. Rev. Lett. **96**, 082003 (2006).
 - [14] H. Albrecht *et al.* [ARGUS Collaboration], Phys. Lett. **B402**, 207-212 (1997).
 - [15] P. L. Frabetti *et al.* [E687 Collaboration], Phys. Lett. **B365**, 461-469 (1996).
 - [16] B. Aubert *et al.* [BABAR Collaboration], Phys. Rev. Lett. **98**, 012001 (2007).
 - [17] K. Abe *et al.* [Belle Collaboration], Phys. Rev. Lett. **98**, 262001 (2007).
 - [18] M. Artuso *et al.* [CLEO Collaboration], Phys. Rev. Lett. **86**, 4479-4482 (2001).
 - [19] H. Albrecht *et al.* [ARGUS Collaboration], Phys. Lett. **B317**, 227-232 (1993).
 - [20] P. L. Frabetti *et al.* [E687 Collaboration], Phys. Rev. Lett. **72**, 961-964 (1994).
 - [21] K. W. Edwards *et al.* [CLEO Collaboration], Phys. Rev. Lett. **74**, 3331-3335 (1995).
 - [22] R. Ammar *et al.* [CLEO Collaboration], Phys. Rev. Lett. **86**, 1167-1170 (2001).
 - [23] G. Brandenburg *et al.* [CLEO Collaboration], Phys. Rev. Lett. **78**, 2304-2308 (1997).
 - [24] V. V. Ammosov, I. L. Vasilev, A. A. Ivanilov, P. V. Ivanov, V. I. Konyushko, V. M. Korablev, V. A. Korotkov, V. V. Ma-
keev *et al.*, JETP Lett. **58**, 247-251 (1993).
 - [25] B. Aubert *et al.* [BABAR Collaboration], Phys. Rev. **D78**, 112003 (2008).
 - [26] R. Mizuk *et al.* [Belle Collaboration], Phys. Rev. Lett. **94**, 122002 (2005).
 - [27] T. Lesiak *et al.* [Belle Collaboration], Phys. Lett. **B665**, 9-15 (2008).
 - [28] P. L. Frabetti *et al.* [The E687 Collaboration], Phys. Lett. **B426**, 403-410 (1998).
 - [29] L. Gibbons *et al.* [CLEO Collaboration], Phys. Rev. Lett. **77**, 810-813 (1996).
 - [30] P. Avery *et al.* [CLEO Collaboration], Phys. Rev. Lett. **75**, 4364-4368 (1995).
 - [31] S. E. Csorna *et al.* [CLEO Collaboration], Phys. Rev. Lett. **86**, 4243-4246 (2001).
 - [32] J. P. Alexander *et al.* [CLEO Collaboration], Phys. Rev. Lett. **83**, 3390-3393 (1999).
 - [33] B. Aubert *et al.* [BABAR Collaboration], Phys. Rev. **D77**, 012002 (2008).
 - [34] R. Chistov *et al.* [BELLE Collaboration], Phys. Rev. Lett. **97**, 162001 (2006).
 - [35] C. P. Jessop *et al.* [CLEO Collaboration], Phys. Rev. Lett. **82**, 492 (1999).
 - [36] B. Aubert *et al.* [BaBar Collaboration], Phys. Rev. Lett. **97**, 232001 (2006).
 - [37] J. Aichelin *et al.*, The CBM Physics Book, Lect. Notes in Phys. **814** (2011) 1-960, eds. B. Friman, C. Hohne, J. Knoll, S.
Leupold, J. Randrup, R. Rapp, and P. Senger (Springer).
 - [38] Physics Performance Report for PANDA: Strong Interaction Studies with Antiprotons, PANDA Collaboration,
arXiv:0903.3905 [http://www.gsi.de/PANDA].
 - [39] N. Kaiser, P. B. Siegel and W. Weise, Nucl. Phys. A **594**, 325 (1995).
 - [40] N. Kaiser, P. B. Siegel and W. Weise, Phys. Lett. B **362**, 23 (1995).
 - [41] E. Oset and A. Ramos, Nucl. Phys. A **635**, 99 (1998).
 - [42] B. Krippa, Phys. Rev. C **58**, 1333 (1998).
 - [43] B. Krippa and J. T. Londergan, Phys. Rev. C **58**, 1634 (1998).
 - [44] J. C. Nacher, A. Parreno, E. Oset, A. Ramos, A. Hosaka and M. Oka, Nucl. Phys. A **678**, 187 (2000).
 - [45] U. G. Meissner and J. A. Oller, Nucl. Phys. A **673**, 311 (2000).
 - [46] J. A. Oller and U. G. Meissner, Phys. Lett. B **500**, 263 (2001).
 - [47] D. Jido, J. A. Oller, E. Oset, A. Ramos and U. G. Meissner, Nucl. Phys. A **725**, 181 (2003).
 - [48] J. Nieves and E. Ruiz Arriola, Phys. Rev. D **64**, 116008 (2001).
 - [49] T. Inoue, E. Oset and M. J. Vicente Vacas, Phys. Rev. C **65**, 035204 (2002).
 - [50] M. F. M. Lutz and E. E. Kolomeitsev, Nucl. Phys. A **700**, 193 (2002).
 - [51] C. Garcia-Recio, J. Nieves, E. Ruiz Arriola and M. J. Vicente Vacas, Phys. Rev. D **67**, 076009 (2003).
 - [52] E. Oset, A. Ramos and C. Bennhold, Phys. Lett. B **527**, 99 (2002) [Erratum-ibid. B **530**, 260 (2002)].
 - [53] A. Ramos, E. Oset and C. Bennhold, Phys. Rev. Lett. **89**, 252001 (2002).
 - [54] L. Tolos, A. Ramos, A. Polls and T. T. S. Kuo, Nucl. Phys. A **690**, 547 (2001).
 - [55] L. Tolos, A. Ramos and A. Polls, Phys. Rev. C **65**, 054907 (2002).

- [56] C. Garcia-Recio, M. F. M. Lutz and J. Nieves, Phys. Lett. B **582**, 49 (2004).
- [57] J. A. Oller, J. Prades and M. Verbeni, Phys. Rev. Lett. **95**, 172502 (2005).
- [58] B. Borasoy, R. Nissler and W. Weise, Eur. Phys. J. A **25**, 79 (2005).
- [59] B. Borasoy, U. G. Meissner and R. Nissler, Phys. Rev. C **74**, 055201 (2006).
- [60] T. Hyodo, D. Jido and A. Hosaka, Phys. Rev. C **78**, 025203 (2008).
- [61] L. Tolos, J. Schaffner-Bielich and A. Mishra, Phys. Rev. C **70**, 025203 (2004).
- [62] L. Tolos, J. Schaffner-Bielich and H. Stoecker, Phys. Lett. B **635**, 85 (2006).
- [63] M. F. M. Lutz and E. E. Kolomeitsev, Nucl. Phys. A **730**, 110 (2004).
- [64] M. F. M. Lutz and E. E. Kolomeitsev, Nucl. Phys. A **755**, 29 (2005).
- [65] J. Hofmann and M. F. M. Lutz, Nucl. Phys. A **763**, 90 (2005).
- [66] J. Hofmann and M. F. M. Lutz, Nucl. Phys. A **776**, 17 (2006).
- [67] M. F. M. Lutz and C. L. Korpa, Phys. Lett. B **633**, 43 (2006).
- [68] T. Mizutani and A. Ramos, Phys. Rev. C **74**, 065201 (2006).
- [69] L. Tolos, A. Ramos and T. Mizutani, Phys. Rev. C **77**, 015207 (2008).
- [70] C. E. Jimenez-Tejero, A. Ramos and I. Vidana, Phys. Rev. C **80**, 055206 (2009).
- [71] J. Haidenbauer, G. Krein, U. G. Meissner and A. Sibirtsev, Eur. Phys. J. A **33**, 107 (2007).
- [72] J. Haidenbauer, G. Krein, U. G. Meissner and A. Sibirtsev, Eur. Phys. J. A **37**, 55 (2008).
- [73] J. Haidenbauer, G. Krein, U. G. Meissner and L. Tolos, Eur. Phys. J. A **47**, 18 (2011).
- [74] J. -J. Wu, R. Molina, E. Oset and B. S. Zou, Phys. Rev. Lett. **105**, 232001 (2010).
- [75] J. -J. Wu, R. Molina, E. Oset and B. S. Zou, Phys. Rev. C **84**, 015202 (2011).
- [76] J. -J. Wu, T. -S. H. Lee and B. S. Zou, Phys. Rev. C **85**, 044002 (2012).
- [77] E. Oset, A. Ramos, E. J. Garzon, R. Molina, L. Tolos, C. W. Xiao, J. J. Wu and B. S. Zou, Int. J. Mod. Phys. E **21**, 1230011 (2012).
- [78] N. Isgur and M. B. Wise, Phys. Lett. B **232**, 113 (1989).
- [79] M. Neubert, Phys. Rept. **245**, 259 (1994).
- [80] A.V. Manohar and M.B. Wise, *Heavy Quark Physics*, Cambridge Monographs on Particle Physics, Nuclear Physics and Cosmology, vol. 10 (2000).
- [81] C. Garcia-Recio, V. K. Magas, T. Mizutani, J. Nieves, A. Ramos, L. L. Salcedo and L. Tolos, Phys. Rev. D **79**, 054004 (2009).
- [82] D. Gamermann, C. Garcia-Recio, J. Nieves, L. L. Salcedo and L. Tolos, Phys. Rev. D **81**, 094016 (2010).
- [83] O. Romanets, L. Tolos, C. Garcia-Recio, J. Nieves, L. L. Salcedo and R. G. E. Timmermans, Phys. Rev. D **85**, 114032 (2012).
- [84] C. Garcia-Recio, J. Nieves and L. L. Salcedo, Phys. Rev. D **74**, 034025 (2006).
- [85] C. Garcia-Recio, J. Nieves and L. L. Salcedo, Phys. Rev. D **74**, 036004 (2006).
- [86] H. Toki, C. Garcia-Recio and J. Nieves, Phys. Rev. D **77**, 034001 (2008).
- [87] D. Gamermann, C. Garcia-Recio, J. Nieves and L. L. Salcedo, Phys. Rev. D **84**, 056017 (2011).
- [88] C. Garcia-Recio, J. Nieves, O. Romanets, L. L. Salcedo and L. Tolos, Phys. Rev. D **87**, 034032 (2013).
- [89] R. Aaij *et al.* [LHCb Collaboration], Phys. Rev. Lett. **109**, 172003 (2012).
- [90] S. Weinberg, Phys. Rev. Lett. **17**, 616 (1966).
- [91] Y. Tomozawa, Nuovo Cim. A **46**, 707 (1966).
- [92] M. C. Birse, Z. Phys. A **355**, 231 (1996).
- [93] F. Mandl and G. Shaw, Chichester, UK: Wiley (1984) 354 p.
- [94] C. Itzykson and J. B. Zuber, New York, USA: McGraw-Hill (1980) 705 P. (International Series in Pure and Applied Physics).
- [95] J. Beringer *et al.* [Particle Data Group Collaboration], Phys. Rev. D **86**, 010001 (2012).
- [96] T. Hyodo, D. Jido and A. Hosaka, Phys. Rev. D **75**, 034002 (2007).
- [97] F. Gursey and L. A. Radicati, Phys. Rev. Lett. **13**, 173 (1964).
- [98] A. Pais, Phys. Rev. Lett. **13**, 175 (1964).
- [99] B. Sakita, Phys. Rev. **136**, B1756 (1964).
- [100] A. J. G. Hey and R. L. Kelly, Phys. Rept. **96**, 71 (1983).
- [101] R. F. Lebed, Phys. Rev. D **51**, 5039 (1995).
- [102] R. F. Dashen, E. E. Jenkins and A. V. Manohar, Phys. Rev. D **49**, 4713 (1994) [Erratum-ibid. D **51**, 2489 (1995)].
- [103] D. G. Caldi and H. Pagels, Phys. Rev. D **14**, 809 (1976).
- [104] D. G. Caldi and H. Pagels, Phys. Rev. D **15**, 2668 (1977).
- [105] R. P. Feynman, M. Gell-Mann and G. Zweig, Phys. Rev. Lett. **13**, 678 (1964).
- [106] J. Smit, Nucl. Phys. B **175**, 307 (1980).
- [107] S. R. Coleman and J. Mandula, Phys. Rev. **159**, 1251 (1967).
- [108] S. Godfrey and N. Isgur, Phys. Rev. D **32**, 189 (1985).
- [109] S. Capstick and N. Isgur, Phys. Rev. D **34**, 2809 (1986).
- [110] C. Garcia-Recio, L. S. Geng, J. Nieves and L. L. Salcedo, Phys. Rev. D **83**, 016007 (2011).
- [111] C. Garcia-Recio and L. L. Salcedo, J. Math. Phys. **52**, 043503 (2011).
- [112] A. F. Falk, H. Georgi, B. Grinstein and M. B. Wise, Nucl. Phys. B **343**, 1 (1990).
- [113] B. Grinstein, E. E. Jenkins, A. V. Manohar, M. J. Savage and M. B. Wise, Nucl. Phys. B **380**, 369 (1992).
- [114] E. E. Jenkins, M. E. Luke, A. V. Manohar and M. J. Savage, Nucl. Phys. B **390**, 463 (1993).
- [115] J. D. Bjorken and S. D. Drell, "Relativistic quantum fields," ISBN-0070054940.

- [116] G. E. Baird and L. C. Biedenharn, J. Math. Phys. **5**, 1723 (1964).
- [117] J. J. de Swart, Rev. Mod. Phys. **35**, 916 (1963) [Erratum-ibid. **37**, 326 (1965)].
- [118] J. J. Dudek, R. G. Edwards and D. G. Richards, Phys. Rev. D **73**, 074507 (2006).
- [119] S. G. Yuan, K. W. Wei, J. He, H. S. Xu and B. S. Zou, Eur. Phys. J. A **48**,61 (2012).

TABLE V: $C = 0, S = 0, I = 1/2, J = 1/2$.

	$N\eta_c$	$N\psi$	$\Lambda_c \bar{D}$	$\Lambda_c \bar{D}^*$	$\Sigma_c \bar{D}$	$\Sigma_c \bar{D}^*$	$\Sigma_c^* \bar{D}^*$
$N\eta_c$	0	0	$\sqrt{\frac{3}{2}}$	$-\sqrt{\frac{9}{2}}$	$\sqrt{\frac{3}{2}}$	$\sqrt{\frac{1}{2}}$	2
$N\psi$	0	0	$-\sqrt{\frac{9}{2}}$	$-\sqrt{\frac{3}{2}}$	$\sqrt{\frac{1}{2}}$	$\sqrt{\frac{25}{6}}$	$-\sqrt{\frac{4}{3}}$
$\Lambda_c \bar{D}$	$\sqrt{\frac{3}{2}}$	$-\sqrt{\frac{9}{2}}$	1	0	0	$-\sqrt{3}$	$\sqrt{6}$
$\Lambda_c \bar{D}^*$	$-\sqrt{\frac{9}{2}}$	$-\sqrt{\frac{3}{2}}$	0	1	$-\sqrt{3}$	-2	$-\sqrt{2}$
$\Sigma_c \bar{D}$	$\sqrt{\frac{3}{2}}$	$\sqrt{\frac{1}{2}}$	0	$-\sqrt{3}$	-1	$\sqrt{\frac{4}{3}}$	$\sqrt{\frac{2}{3}}$
$\Sigma_c \bar{D}^*$	$\sqrt{\frac{1}{2}}$	$\sqrt{\frac{25}{6}}$	$-\sqrt{3}$	-2	$\sqrt{\frac{4}{3}}$	$\frac{1}{3}$	$-\sqrt{\frac{2}{9}}$
$\Sigma_c^* \bar{D}^*$	2	$-\sqrt{\frac{4}{3}}$	$\sqrt{6}$	$-\sqrt{2}$	$\sqrt{\frac{2}{3}}$	$-\sqrt{\frac{2}{9}}$	$\frac{2}{3}$

TABLE VI: $C = 0, S = 0, I = 1/2, J = 3/2$.

	$N\psi$	$\Lambda_c \bar{D}^*$	$\Sigma_c^* \bar{D}$	$\Sigma_c \bar{D}^*$	$\Sigma_c^* \bar{D}^*$
$N\psi$	0	$\sqrt{6}$	$-\sqrt{2}$	$\sqrt{\frac{2}{3}}$	$-\sqrt{\frac{10}{3}}$
$\Lambda_c \bar{D}^*$	$\sqrt{6}$	1	$-\sqrt{3}$	1	$-\sqrt{5}$
$\Sigma_c^* \bar{D}$	$-\sqrt{2}$	$-\sqrt{3}$	-1	$-\sqrt{\frac{1}{3}}$	$\sqrt{\frac{5}{3}}$
$\Sigma_c \bar{D}^*$	$\sqrt{\frac{2}{3}}$	1	$-\sqrt{\frac{1}{3}}$	$-\frac{5}{3}$	$-\sqrt{\frac{5}{9}}$
$\Sigma_c^* \bar{D}^*$	$-\sqrt{\frac{10}{3}}$	$-\sqrt{5}$	$\sqrt{\frac{5}{3}}$	$-\sqrt{\frac{5}{9}}$	$-\frac{1}{3}$

TABLE VIII: $C = 0, S = 0, I = 3/2, J = 1/2$.

	$\Delta\psi$	$\Sigma_c \bar{D}$	$\Sigma_c \bar{D}^*$	$\Sigma_c^* \bar{D}^*$
$\Delta\psi$	0	$\sqrt{8}$	$-\sqrt{\frac{8}{3}}$	$-\sqrt{\frac{4}{3}}$
$\Sigma_c \bar{D}$	$\sqrt{8}$	2	$-\sqrt{\frac{16}{3}}$	$-\sqrt{\frac{8}{3}}$
$\Sigma_c \bar{D}^*$	$-\sqrt{\frac{8}{3}}$	$-\sqrt{\frac{16}{3}}$	$-\frac{2}{3}$	$\sqrt{\frac{8}{9}}$
$\Sigma_c^* \bar{D}^*$	$-\sqrt{\frac{4}{3}}$	$-\sqrt{\frac{8}{3}}$	$\sqrt{\frac{8}{9}}$	$-\frac{4}{3}$

TABLE IX: $C = 0, S = 0, I = 3/2, J = 3/2$.

	$\Delta\eta_c$	$\Delta\psi$	$\Sigma_c^* \bar{D}$	$\Sigma_c \bar{D}^*$	$\Sigma_c^* \bar{D}^*$
$\Delta\eta_c$	0	0	$\sqrt{3}$	-2	$-\sqrt{5}$
$\Delta\psi$	0	0	$-\sqrt{5}$	$-\sqrt{\frac{20}{3}}$	$\sqrt{\frac{1}{3}}$
$\Sigma_c^* \bar{D}$	$\sqrt{3}$	$-\sqrt{5}$	2	$\sqrt{\frac{4}{3}}$	$-\sqrt{\frac{20}{3}}$
$\Sigma_c \bar{D}^*$	-2	$-\sqrt{\frac{20}{3}}$	$\sqrt{\frac{4}{3}}$	$\frac{10}{3}$	$\sqrt{\frac{20}{9}}$
$\Sigma_c^* \bar{D}^*$	$-\sqrt{5}$	$\sqrt{\frac{1}{3}}$	$-\sqrt{\frac{20}{3}}$	$\sqrt{\frac{20}{9}}$	$\frac{2}{3}$

TABLE X: $C = 0, S = 0, I = 3/2, J = 5/2$.

	$\Delta\psi$	$\Sigma_c^* \bar{D}^*$
$\Delta\psi$	0	$\sqrt{12}$
$\Sigma_c^* \bar{D}^*$	$\sqrt{12}$	4

TABLE VII: $C = 0, S = 0, I = 1/2, J = 5/2$.

	$\Sigma_c^* \bar{D}^*$
$\Sigma_c^* \bar{D}^*$	-2

TABLE XI: $C = 0, S = -1, I = 0, J = 1/2$.

	$\Lambda\eta_c$	$\Lambda\psi$	$\Lambda_c\bar{D}_s$	$\Xi_c\bar{D}$	$\Lambda_c\bar{D}_s^*$	$\Xi'_c\bar{D}$	$\Xi_c\bar{D}^*$	$\Xi'_c\bar{D}^*$	$\Xi_c^*\bar{D}^*$
$\Lambda\eta_c$	0	0	1	$\sqrt{\frac{1}{2}}$	$-\sqrt{3}$	$\sqrt{\frac{3}{2}}$	$-\sqrt{\frac{3}{2}}$	$\sqrt{\frac{1}{2}}$	2
$\Lambda\psi$	0	0	$-\sqrt{3}$	$-\sqrt{\frac{3}{2}}$	-1	$\sqrt{\frac{1}{2}}$	$-\sqrt{\frac{1}{2}}$	$\sqrt{\frac{25}{6}}$	$-\sqrt{\frac{4}{3}}$
$\Lambda_c\bar{D}_s$	1	$-\sqrt{3}$	0	$\sqrt{2}$	0	0	0	$-\sqrt{2}$	2
$\Xi_c\bar{D}$	$\sqrt{\frac{1}{2}}$	$-\sqrt{\frac{3}{2}}$	$\sqrt{2}$	-1	0	0	0	-1	$\sqrt{2}$
$\Lambda_c\bar{D}_s^*$	$-\sqrt{3}$	-1	0	0	0	$-\sqrt{2}$	$\sqrt{2}$	$-\sqrt{\frac{8}{3}}$	$-\sqrt{\frac{4}{3}}$
$\Xi'_c\bar{D}$	$\sqrt{\frac{3}{2}}$	$\sqrt{\frac{1}{2}}$	0	0	$-\sqrt{2}$	-1	-1	$\sqrt{\frac{4}{3}}$	$\sqrt{\frac{2}{3}}$
$\Xi_c\bar{D}^*$	$-\sqrt{\frac{3}{2}}$	$-\sqrt{\frac{1}{2}}$	0	0	$\sqrt{2}$	-1	-1	$-\sqrt{\frac{4}{3}}$	$-\sqrt{\frac{2}{3}}$
$\Xi'_c\bar{D}^*$	$\sqrt{\frac{1}{2}}$	$\sqrt{\frac{25}{6}}$	$-\sqrt{2}$	-1	$-\sqrt{\frac{8}{3}}$	$\sqrt{\frac{4}{3}}$	$-\sqrt{\frac{4}{3}}$	$\frac{1}{3}$	$-\sqrt{\frac{2}{9}}$
$\Xi_c^*\bar{D}^*$	2	$-\sqrt{\frac{4}{3}}$	2	$\sqrt{2}$	$-\sqrt{\frac{4}{3}}$	$\sqrt{\frac{2}{3}}$	$-\sqrt{\frac{2}{3}}$	$-\sqrt{\frac{2}{9}}$	$\frac{2}{3}$

TABLE XII: $C = 0, S = -1, I = 0, J = 3/2$.

	$\Lambda\psi$	$\Lambda_c\bar{D}_s^*$	$\Xi_c\bar{D}^*$	$\Xi'_c\bar{D}$	$\Xi'_c\bar{D}^*$	$\Xi_c^*\bar{D}^*$
$\Lambda\psi$	0	2	$\sqrt{2}$	$-\sqrt{2}$	$\sqrt{\frac{2}{3}}$	$-\sqrt{\frac{10}{3}}$
$\Lambda_c\bar{D}_s^*$	2	0	$\sqrt{2}$	$-\sqrt{2}$	$\sqrt{\frac{2}{3}}$	$-\sqrt{\frac{10}{3}}$
$\Xi_c\bar{D}^*$	$\sqrt{2}$	$\sqrt{2}$	-1	-1	$\sqrt{\frac{1}{3}}$	$-\sqrt{\frac{5}{3}}$
$\Xi'_c\bar{D}$	$-\sqrt{2}$	$-\sqrt{2}$	-1	-1	$-\sqrt{\frac{1}{3}}$	$\sqrt{\frac{5}{3}}$
$\Xi'_c\bar{D}^*$	$\sqrt{\frac{2}{3}}$	$\sqrt{\frac{2}{3}}$	$\sqrt{\frac{1}{3}}$	$-\sqrt{\frac{1}{3}}$	$-\frac{5}{3}$	$-\sqrt{\frac{5}{9}}$
$\Xi_c^*\bar{D}^*$	$-\sqrt{\frac{10}{3}}$	$-\sqrt{\frac{10}{3}}$	$-\sqrt{\frac{5}{3}}$	$\sqrt{\frac{5}{3}}$	$-\sqrt{\frac{5}{9}}$	$-\frac{1}{3}$

TABLE XIII: $C = 0, S = -1, I = 0, J = 5/2$.

	$\Xi_c^*\bar{D}^*$
$\Xi_c^*\bar{D}^*$	-2

TABLE XIV: $C = 0, S = -1, I = 1, J = 1/2$.

	$\Sigma\eta_c$	$\Sigma\psi$	$\Xi_c\bar{D}$	$\Sigma_c\bar{D}_s$	$\Xi'_c\bar{D}$	$\Xi_c\bar{D}^*$	$\Sigma^*\psi$	$\Sigma_c\bar{D}_s^*$	$\Xi'_c\bar{D}^*$	$\Sigma_c^*\bar{D}_s^*$	$\Xi_c^*\bar{D}^*$
$\Sigma\eta_c$	0	0	$\sqrt{\frac{3}{2}}$	1	$-\sqrt{\frac{1}{2}}$	$-\sqrt{\frac{9}{2}}$	0	$\sqrt{\frac{1}{3}}$	$-\sqrt{\frac{1}{6}}$	$\sqrt{\frac{8}{3}}$	$-\sqrt{\frac{4}{3}}$
$\Sigma\psi$	0	0	$-\sqrt{\frac{9}{2}}$	$\sqrt{\frac{1}{3}}$	$-\sqrt{\frac{1}{6}}$	$-\sqrt{\frac{3}{2}}$	0	$\frac{5}{3}$	$-\sqrt{\frac{25}{18}}$	$-\sqrt{\frac{8}{9}}$	$\frac{2}{3}$
$\Xi_c\bar{D}$	$\sqrt{\frac{3}{2}}$	$-\sqrt{\frac{9}{2}}$	1	0	0	0	0	$-\sqrt{2}$	1	2	$-\sqrt{2}$
$\Sigma_c\bar{D}_s$	1	$\sqrt{\frac{1}{3}}$	0	0	$\sqrt{2}$	$-\sqrt{2}$	$\sqrt{\frac{8}{3}}$	0	$-\sqrt{\frac{8}{3}}$	0	$-\sqrt{\frac{4}{3}}$
$\Xi'_c\bar{D}$	$-\sqrt{\frac{1}{2}}$	$-\sqrt{\frac{1}{6}}$	0	$\sqrt{2}$	1	1	$\sqrt{\frac{16}{3}}$	$-\sqrt{\frac{8}{3}}$	$-\sqrt{\frac{4}{3}}$	$-\sqrt{\frac{4}{3}}$	$-\sqrt{\frac{2}{3}}$
$\Xi_c\bar{D}^*$	$-\sqrt{\frac{9}{2}}$	$-\sqrt{\frac{3}{2}}$	0	$-\sqrt{2}$	1	1	0	$-\sqrt{\frac{8}{3}}$	$\sqrt{\frac{4}{3}}$	$-\sqrt{\frac{4}{3}}$	$\sqrt{\frac{2}{3}}$
$\Sigma^*\psi$	0	0	0	$\sqrt{\frac{8}{3}}$	$\sqrt{\frac{16}{3}}$	0	0	$-\sqrt{\frac{8}{9}}$	$-\frac{4}{3}$	$-\frac{2}{3}$	$-\sqrt{\frac{8}{9}}$
$\Sigma_c\bar{D}_s^*$	$\sqrt{\frac{1}{3}}$	$\frac{5}{3}$	$-\sqrt{2}$	0	$-\sqrt{\frac{8}{3}}$	$-\sqrt{\frac{8}{3}}$	$-\sqrt{\frac{8}{9}}$	0	$-\sqrt{\frac{2}{9}}$	0	$\frac{2}{3}$
$\Xi'_c\bar{D}^*$	$-\sqrt{\frac{1}{6}}$	$-\sqrt{\frac{25}{18}}$	1	$-\sqrt{\frac{8}{3}}$	$-\sqrt{\frac{4}{3}}$	$\sqrt{\frac{4}{3}}$	$-\frac{4}{3}$	$-\sqrt{\frac{2}{9}}$	$-\frac{1}{3}$	$\frac{2}{3}$	$\sqrt{\frac{2}{9}}$
$\Sigma_c^*\bar{D}_s^*$	$\sqrt{\frac{8}{3}}$	$-\sqrt{\frac{8}{9}}$	2	0	$-\sqrt{\frac{4}{3}}$	$-\sqrt{\frac{4}{3}}$	$-\frac{2}{3}$	0	$\frac{2}{3}$	0	$-\sqrt{\frac{8}{9}}$
$\Xi_c^*\bar{D}^*$	$-\sqrt{\frac{4}{3}}$	$\frac{2}{3}$	$-\sqrt{2}$	$-\sqrt{\frac{4}{3}}$	$-\sqrt{\frac{2}{3}}$	$\sqrt{\frac{2}{3}}$	$-\sqrt{\frac{8}{9}}$	$\frac{2}{3}$	$\sqrt{\frac{2}{9}}$	$-\sqrt{\frac{8}{9}}$	$-\frac{2}{3}$

TABLE XV: $C = 0, S = -1, I = 1, J = 3/2$.

	$\Sigma\psi$	$\Sigma^*\eta_c$	$\Xi_c\bar{D}^*$	$\Sigma^*\psi$	$\Sigma_c^*\bar{D}_s$	$\Xi_c^*\bar{D}$	$\Sigma_c\bar{D}_s^*$	$\Xi_c'\bar{D}^*$	$\Sigma_c^*\bar{D}_s^*$	$\Xi_c^*\bar{D}^*$
$\Sigma\psi$	0	0	$\sqrt{6}$	0	$-\sqrt{\frac{4}{3}}$	$\sqrt{\frac{2}{3}}$	$\frac{2}{3}$	$-\sqrt{\frac{2}{9}}$	$-\sqrt{\frac{20}{9}}$	$\sqrt{\frac{10}{9}}$
$\Sigma^*\eta_c$	0	0	0	0	1	$\sqrt{2}$	$-\sqrt{\frac{4}{3}}$	$-\sqrt{\frac{8}{3}}$	$-\sqrt{\frac{5}{3}}$	$-\sqrt{\frac{10}{3}}$
$\Xi_c\bar{D}^*$	$\sqrt{6}$	0	1	0	$-\sqrt{2}$	1	$\sqrt{\frac{2}{3}}$	$-\sqrt{\frac{1}{3}}$	$-\sqrt{\frac{10}{3}}$	$\sqrt{\frac{5}{3}}$
$\Sigma^*\psi$	0	0	0	0	$-\sqrt{\frac{5}{3}}$	$-\sqrt{\frac{10}{3}}$	$-\sqrt{\frac{20}{9}}$	$-\sqrt{\frac{40}{9}}$	$\frac{1}{3}$	$\sqrt{\frac{2}{9}}$
$\Sigma_c^*\bar{D}_s$	$-\sqrt{\frac{4}{3}}$	1	$-\sqrt{2}$	$-\sqrt{\frac{5}{3}}$	0	$\sqrt{2}$	0	$\sqrt{\frac{2}{3}}$	0	$-\sqrt{\frac{10}{3}}$
$\Xi_c^*\bar{D}$	$\sqrt{\frac{2}{3}}$	$\sqrt{2}$	1	$-\sqrt{\frac{10}{3}}$	$\sqrt{2}$	1	$\sqrt{\frac{2}{3}}$	$\sqrt{\frac{1}{3}}$	$-\sqrt{\frac{10}{3}}$	$-\sqrt{\frac{5}{3}}$
$\Sigma_c\bar{D}_s^*$	$\frac{2}{3}$	$-\sqrt{\frac{4}{3}}$	$\sqrt{\frac{2}{3}}$	$-\sqrt{\frac{20}{9}}$	0	$\sqrt{\frac{2}{3}}$	0	$\sqrt{\frac{50}{9}}$	0	$\sqrt{\frac{10}{9}}$
$\Xi_c'\bar{D}^*$	$-\sqrt{\frac{2}{9}}$	$-\sqrt{\frac{8}{3}}$	$-\sqrt{\frac{1}{3}}$	$-\sqrt{\frac{40}{9}}$	$\sqrt{\frac{2}{3}}$	$\sqrt{\frac{1}{3}}$	$\sqrt{\frac{50}{9}}$	$\frac{5}{3}$	$\sqrt{\frac{10}{9}}$	$\sqrt{\frac{5}{9}}$
$\Sigma_c^*\bar{D}_s^*$	$-\sqrt{\frac{20}{9}}$	$-\sqrt{\frac{5}{3}}$	$-\sqrt{\frac{10}{3}}$	$\frac{1}{3}$	0	$-\sqrt{\frac{10}{3}}$	0	$\sqrt{\frac{10}{9}}$	0	$\sqrt{\frac{2}{9}}$
$\Xi_c^*\bar{D}^*$	$\sqrt{\frac{10}{9}}$	$-\sqrt{\frac{10}{3}}$	$\sqrt{\frac{5}{3}}$	$\sqrt{\frac{2}{9}}$	$-\sqrt{\frac{10}{3}}$	$-\sqrt{\frac{5}{3}}$	$\sqrt{\frac{10}{9}}$	$\sqrt{\frac{5}{9}}$	$\sqrt{\frac{2}{9}}$	$\frac{1}{3}$

TABLE XVI: $C = 0, S = -1, I = 1, J = 5/2$.

	$\Sigma^*\psi$	$\Sigma_c^*\bar{D}_s^*$	$\Xi_c^*\bar{D}^*$
$\Sigma^*\psi$	0	2	$\sqrt{8}$
$\Sigma_c^*\bar{D}_s^*$	2	0	$\sqrt{8}$
$\Xi_c^*\bar{D}^*$	$\sqrt{8}$	$\sqrt{8}$	2

TABLE XVII: $C = 0, S = -2, I = 1/2, J = 1/2$.

	$\Xi\eta_c$	$\Xi\psi$	$\Xi_c\bar{D}_s$	$\Xi_c'\bar{D}_s$	$\Omega_c\bar{D}$	$\Xi_c\bar{D}_s^*$	$\Xi^*\psi$	$\Xi_c'\bar{D}_s^*$	$\Omega_c\bar{D}^*$	$\Xi_c^*\bar{D}_s^*$	$\Omega_c^*\bar{D}^*$
$\Xi\eta_c$	0	0	$\sqrt{\frac{3}{2}}$	$\sqrt{\frac{1}{2}}$	-1	$-\sqrt{\frac{9}{2}}$	0	$\sqrt{\frac{1}{6}}$	$-\sqrt{\frac{1}{3}}$	$\sqrt{\frac{4}{3}}$	$-\sqrt{\frac{8}{3}}$
$\Xi\psi$	0	0	$-\sqrt{\frac{9}{2}}$	$\sqrt{\frac{1}{6}}$	$-\sqrt{\frac{1}{3}}$	$-\sqrt{\frac{3}{2}}$	0	$\sqrt{\frac{25}{18}}$	$-\frac{5}{3}$	$-\frac{2}{3}$	$\sqrt{\frac{8}{9}}$
$\Xi_c\bar{D}_s$	$\sqrt{\frac{3}{2}}$	$-\sqrt{\frac{9}{2}}$	1	0	0	0	0	-1	$\sqrt{2}$	$\sqrt{2}$	-2
$\Xi_c'\bar{D}_s$	$\sqrt{\frac{1}{2}}$	$\sqrt{\frac{1}{6}}$	0	1	$\sqrt{2}$	-1	$\sqrt{\frac{16}{3}}$	$-\sqrt{\frac{4}{3}}$	$-\sqrt{\frac{8}{3}}$	$-\sqrt{\frac{2}{3}}$	$-\sqrt{\frac{4}{3}}$
$\Omega_c\bar{D}$	-1	$-\sqrt{\frac{1}{3}}$	0	$\sqrt{2}$	0	$\sqrt{2}$	$\sqrt{\frac{8}{3}}$	$-\sqrt{\frac{8}{3}}$	0	$-\sqrt{\frac{4}{3}}$	0
$\Xi_c\bar{D}_s^*$	$-\sqrt{\frac{9}{2}}$	$-\sqrt{\frac{3}{2}}$	0	-1	$\sqrt{2}$	1	0	$-\sqrt{\frac{4}{3}}$	$\sqrt{\frac{8}{3}}$	$-\sqrt{\frac{2}{3}}$	$\sqrt{\frac{4}{3}}$
$\Xi^*\psi$	0	0	0	$\sqrt{\frac{16}{3}}$	$\sqrt{\frac{8}{3}}$	0	0	$-\frac{4}{3}$	$-\sqrt{\frac{8}{9}}$	$-\sqrt{\frac{8}{9}}$	$-\frac{2}{3}$
$\Xi_c'\bar{D}_s^*$	$\sqrt{\frac{1}{6}}$	$\sqrt{\frac{25}{18}}$	-1	$-\sqrt{\frac{4}{3}}$	$-\sqrt{\frac{8}{3}}$	$-\sqrt{\frac{4}{3}}$	$-\frac{4}{3}$	$-\frac{1}{3}$	$-\sqrt{\frac{2}{9}}$	$\sqrt{\frac{2}{9}}$	$\frac{2}{3}$
$\Omega_c\bar{D}^*$	$-\sqrt{\frac{1}{3}}$	$-\frac{5}{3}$	$\sqrt{2}$	$-\sqrt{\frac{8}{3}}$	0	$\sqrt{\frac{8}{3}}$	$-\sqrt{\frac{8}{9}}$	$-\sqrt{\frac{2}{9}}$	0	$\frac{2}{3}$	0
$\Xi_c^*\bar{D}_s^*$	$\sqrt{\frac{4}{3}}$	$-\frac{2}{3}$	$\sqrt{2}$	$-\sqrt{\frac{2}{3}}$	$-\sqrt{\frac{4}{3}}$	$-\sqrt{\frac{2}{3}}$	$\sqrt{\frac{2}{9}}$	$\frac{2}{3}$	$-\frac{2}{3}$	$-\sqrt{\frac{8}{9}}$	$-\sqrt{\frac{8}{9}}$
$\Omega_c^*\bar{D}^*$	$-\sqrt{\frac{8}{3}}$	$\sqrt{\frac{8}{9}}$	-2	$-\sqrt{\frac{4}{3}}$	0	$\sqrt{\frac{4}{3}}$	$-\frac{2}{3}$	$\frac{2}{3}$	0	$-\sqrt{\frac{8}{9}}$	0

TABLE XVIII: $C = 0, S = -2, I = 1/2, J = 3/2$.

	$\Xi\psi$	$\Xi^*\eta_c$	$\Xi_c\bar{D}_s^*$	$\Xi_c^*\bar{D}_s$	$\Xi^*\psi$	$\Omega_c^*\bar{D}$	$\Xi_c'\bar{D}_s^*$	$\Omega_c\bar{D}^*$	$\Xi_c^*\bar{D}_s^*$	$\Omega_c^*\bar{D}^*$
$\Xi\psi$	0	0	$\sqrt{6}$	$-\sqrt{\frac{2}{3}}$	0	$\sqrt{\frac{4}{3}}$	$\sqrt{\frac{2}{9}}$	$-\frac{2}{3}$	$-\sqrt{\frac{10}{9}}$	$\sqrt{\frac{20}{9}}$
$\Xi^*\eta_c$	0	0	0	$\sqrt{2}$	0	1	$-\sqrt{\frac{8}{3}}$	$-\sqrt{\frac{4}{3}}$	$-\sqrt{\frac{10}{3}}$	$-\sqrt{\frac{5}{3}}$
$\Xi_c\bar{D}_s^*$	$\sqrt{6}$	0	1	-1	0	$\sqrt{2}$	$\sqrt{\frac{1}{3}}$	$-\sqrt{\frac{2}{3}}$	$-\sqrt{\frac{5}{3}}$	$\sqrt{\frac{10}{3}}$
$\Xi_c^*\bar{D}_s$	$-\sqrt{\frac{2}{3}}$	$\sqrt{2}$	-1	1	$-\sqrt{\frac{10}{3}}$	$\sqrt{2}$	$\sqrt{\frac{1}{3}}$	$\sqrt{\frac{2}{3}}$	$-\sqrt{\frac{5}{3}}$	$-\sqrt{\frac{10}{3}}$
$\Xi^*\psi$	0	0	0	$-\sqrt{\frac{10}{3}}$	0	$-\sqrt{\frac{5}{3}}$	$-\sqrt{\frac{40}{9}}$	$-\sqrt{\frac{20}{9}}$	$\sqrt{\frac{2}{9}}$	$\frac{1}{3}$
$\Omega_c^*\bar{D}$	$\sqrt{\frac{4}{3}}$	1	$\sqrt{2}$	$\sqrt{2}$	$-\sqrt{\frac{5}{3}}$	0	$\sqrt{\frac{2}{3}}$	0	$-\sqrt{\frac{10}{3}}$	0
$\Xi_c'\bar{D}_s^*$	$\sqrt{\frac{2}{9}}$	$-\sqrt{\frac{8}{3}}$	$\sqrt{\frac{1}{3}}$	$\sqrt{\frac{1}{3}}$	$-\sqrt{\frac{40}{9}}$	$\sqrt{\frac{2}{3}}$	$\frac{5}{3}$	$\sqrt{\frac{50}{9}}$	$\sqrt{\frac{5}{9}}$	$\sqrt{\frac{10}{9}}$
$\Omega_c\bar{D}^*$	$-\frac{2}{3}$	$-\sqrt{\frac{4}{3}}$	$-\sqrt{\frac{2}{3}}$	$\sqrt{\frac{2}{3}}$	$-\sqrt{\frac{20}{9}}$	0	$\sqrt{\frac{50}{9}}$	0	$\sqrt{\frac{10}{9}}$	0
$\Xi_c^*\bar{D}_s^*$	$-\sqrt{\frac{10}{9}}$	$-\sqrt{\frac{10}{3}}$	$-\sqrt{\frac{5}{3}}$	$-\sqrt{\frac{5}{3}}$	$\sqrt{\frac{2}{9}}$	$-\sqrt{\frac{10}{3}}$	$\sqrt{\frac{5}{9}}$	$\sqrt{\frac{10}{9}}$	$\frac{1}{3}$	$\sqrt{\frac{2}{9}}$
$\Omega_c^*\bar{D}^*$	$\sqrt{\frac{20}{9}}$	$-\sqrt{\frac{5}{3}}$	$\sqrt{\frac{10}{3}}$	$-\sqrt{\frac{10}{3}}$	$\frac{1}{3}$	0	$\sqrt{\frac{10}{9}}$	0	$\sqrt{\frac{2}{9}}$	0

TABLE XIX: $C = 0, S = -2, I = 1/2, J = 5/2$.

	$\Xi^*\psi$	$\Xi_c^*\bar{D}_s^*$	$\Omega_c^*\bar{D}^*$
$\Xi^*\psi$	0	$\sqrt{8}$	2
$\Xi_c^*\bar{D}_s^*$	$\sqrt{8}$	2	$\sqrt{8}$
$\Omega_c^*\bar{D}^*$	2	$\sqrt{8}$	0

TABLE XX: $C = 0, S = -3, I = 0, J = 1/2$.

	$\Omega_c\bar{D}_s$	$\Omega\psi$	$\Omega_c\bar{D}_s^*$	$\Omega_c^*\bar{D}_s^*$
$\Omega_c\bar{D}_s$	2	$\sqrt{8}$	$-\sqrt{\frac{16}{3}}$	$-\sqrt{\frac{8}{3}}$
$\Omega\psi$	$\sqrt{8}$	0	$-\sqrt{\frac{8}{3}}$	$-\sqrt{\frac{4}{3}}$
$\Omega_c\bar{D}_s^*$	$-\sqrt{\frac{16}{3}}$	$-\sqrt{\frac{8}{3}}$	$-\frac{2}{3}$	$\sqrt{\frac{8}{9}}$
$\Omega_c^*\bar{D}_s^*$	$-\sqrt{\frac{8}{3}}$	$-\sqrt{\frac{4}{3}}$	$\sqrt{\frac{8}{9}}$	$-\frac{4}{3}$

TABLE XXI: $C = 0, S = -3, I = 0, J = 3/2$.

	$\Omega\eta_c$	$\Omega_c^*\bar{D}_s$	$\Omega\psi$	$\Omega_c\bar{D}_s^*$	$\Omega_c^*\bar{D}_s^*$
$\Omega\eta_c$	0	$\sqrt{3}$	0	-2	$-\sqrt{5}$
$\Omega_c^*\bar{D}_s$	$\sqrt{3}$	2	$-\sqrt{5}$	$\sqrt{\frac{4}{3}}$	$-\sqrt{\frac{20}{3}}$
$\Omega\psi$	0	$-\sqrt{5}$	0	$-\sqrt{\frac{20}{3}}$	$\sqrt{\frac{1}{3}}$
$\Omega_c\bar{D}_s^*$	-2	$\sqrt{\frac{4}{3}}$	$-\sqrt{\frac{20}{3}}$	$\frac{10}{3}$	$\sqrt{\frac{20}{9}}$
$\Omega_c^*\bar{D}_s^*$	$-\sqrt{5}$	$-\sqrt{\frac{20}{3}}$	$\sqrt{\frac{1}{3}}$	$\sqrt{\frac{20}{9}}$	$\frac{2}{3}$

TABLE XXII: $C = 0, S = -3, I = 0, J = 5/2$.

	$\Omega\psi$	$\Omega_c^*\bar{D}_s^*$
$\Omega\psi$	0	$\sqrt{12}$
$\Omega_c^*\bar{D}_s^*$	$\sqrt{12}$	4